DETERIORATION OF GREEN CONFLICT PAINT FOR BICYCLE FACILITIES

FINAL PROJECT REPORT

by

Emad Kassem, Michael Lowry, Ebenezer Fanijo, and Maged Mohamed
University of Idaho

Sponsorship
PacTrans

for

Pacific Northwest Transportation Consortium (PacTrans)
USDOT University Transportation Center for Federal Region 10
University of Washington
More Hall 112, Box 352700
Seattle, WA 98195-2700

In cooperation with U.S. Department of Transportation,
Research and Innovative Technology Administration (RITA)

Disclaimer

The contents of this report reflect the views of the authors, who are responsible for the facts and the accuracy of the information presented herein. This document is disseminated under the sponsorship of the U.S. Department of Transportation's University Transportation Centers Program, in the interest of information exchange. The Pacific Northwest Transportation Consortium, the U.S. Government and matching sponsor assume no liability for the contents or use thereof.

Technical Report Documentation Page		
1. Report No.	**2. Government Accession No.** 01701501	**3. Recipient's Catalog No.**
4. Title and Subtitle Deterioration of Green Conflict Paint for Bicycle Facilities		**5. Report Date** February 2021 **6. Performing Organization Code**
7. Author(s) and Affiliations Emad Kassem, 0000-0002-4331-6692; Michael Lowry, 0000-0002-6203-1502; Ebenezer Fanijo, and Maged Mohamed University of Idaho Moscow, ID 83844-1022		**8. Performing Organization Report No.** 2018-S-UI-2
9. Performing Organization Name and Address PacTrans Pacific Northwest Transportation Consortium University Transportation Center for Federal Region 10 University of Washington More Hall 112 Seattle, WA 98195-2700		**10. Work Unit No. (TRAIS)** **11. Contract or Grant No.** 69A3551747110
12. Sponsoring Organization Name and Address United States Department of Transportation Research and Innovative Technology Administration 1200 New Jersey Avenue, SE Washington, DC 20590		**13. Type of Report and Period Covered** **14. Sponsoring Agency Code**
15. Supplementary Notes Report uploaded to: www.pactrans.org		

16. Abstract

Bicyclists depend on the visibility of the surrounding environment to maintain a safe travel path. Throughout the country, new types of bicycle infrastructure and pavement markings are being installed. This study used a new procedure to evaluate different pavement markings used in bike lanes. Three different paints were evaluated, including green waterborne paint, green liquid methacrylate paint, and white thermoplastic paint. The deterioration of these materials was tested under different conditions to simulate wear from motorized vehicles and street equipment. Surface polishing (i.e., repeated passing over the material) was examined under pneumatic tires, steel wheels, and steel scraper blades. Different characteristics were measured, including durability, retroreflectivity, color changes, and friction of the test materials.

The results demonstrated that the procedure used in this study was able to evaluate different materials in a shorter time than field evaluation, which often can take years to complete. As expected, = retroreflectivity decreased with the number of polishing cycles. Overall, there was a significant decrease in percentage of retroreflectivity after 1,000 cycles for all testing conditions before retroreflectivity reached a terminal value. These results were consistent with field observations. A logarithmic model was found to describe the change in the retroreflectivity versus the number of loading cycles with high R^2-values. The methacrylate paint experienced the lowest color loss, even after 100,000 cycles, irrespective of the exposure and the testing conditions. It is believed that the small reduction in color was due to the presence of chemicals coupled with the thicker paint of the methacrylate materials in comparison to the thickness of the waterborne materials. The durability results demonstrated that the waterborne markings peeled off the surface with increasing numbers of polishing cycles.

17. Key Words Bike lanes, pavement markings, MMA, waterborne, retroreflectivity, durability, friction, color change		**18. Distribution Statement**	
19. Security Classification (of this report) Unclassified.	**20. Security Classification (of this page)** Unclassified.	**21. No. of Pages** 46	**22. Price** N/A

Form DOT F 1700.7 (8-72) **Reproduction of completed page authorized.**

SI* (Modern Metric) Conversion Factors

Symbol	When You Know	Multiply By	To Find	Symbol
APPROXIMATE CONVERSIONS TO SI UNITS				
LENGTH				
in	inches	25.4	millimeters	mm
ft	feet	0.305	meters	m
yd	yards	0.914	meters	m
mi	miles	1.61	kilometers	km
AREA				
in^2	square inches	645.2	square millimeters	mm^2
ft^2	square feet	0.093	square meters	m^2
yd^2	square yard	0.836	square meters	m^2
ac	acres	0.405	hectares	ha
mi^2	square miles	2.59	square kilometers	km^2
VOLUME				
fl oz	fluid ounces	29.57	milliliters	mL
gal	gallons	3.785	liters	L
ft^3	cubic feet	0.028	cubic meters	m^3
yd^3	cubic yards	0.765	cubic meters	m^3
NOTE: volumes greater than 1000 L shall be shown in m^3				
MASS				
oz	ounces	28.35	grams	g
lb	pounds	0.454	kilograms	kg
T	short tons (2000 lb)	0.907	megagrams (or "metric ton")	Mg (or "t")
TEMPERATURE (exact degrees)				
°F	Fahrenheit	5 (F-32)/9 or (F-32)/1.8	Celsius	°C
ILLUMINATION				
fc	foot-candles	10.76	lux	lx
fl	foot-Lamberts	3.426	candela/m^2	cd/m^2
FORCE and PRESSURE or STRESS				
lbf	poundforce	4.45	newtons	N
lbf/in^2	poundforce per square inch	6.89	kilopascals	kPa

Symbol	When You Know	Multiply By	To Find	Symbol
APPROXIMATE CONVERSIONS FROM SI UNITS				
LENGTH				
mm	millimeters	0.039	inches	in
m	meters	3.28	feet	ft
m	meters	1.09	yards	yd
km	kilometers	0.621	miles	mi
AREA				
mm^2	square millimeters	0.0016	square inches	in^2
m^2	square meters	10.764	square feet	ft^2
m^2	square meters	1.195	square yards	yd^2
ha	hectares	2.47	acres	ac
km^2	square kilometers	0.386	square miles	mi^2
VOLUME				
mL	milliliters	0.034	fluid ounces	fl oz
L	liters	0.264	gallons	gal
m^3	cubic meters	35.314	cubic feet	ft^3
m^3	cubic meters	1.307	cubic yards	yd^3
MASS				
g	grams	0.035	ounces	oz
kg	kilograms	2.202	pounds	lb
Mg (or "t")	megagrams (or "metric ton")	1.103	short tons (2000 lb)	T
TEMPERATURE (exact degrees)				
°C	Celsius	1.8C+32	Fahrenheit	°F
ILLUMINATION				
lx	lux	0.0929	foot-candles	fc
cd/m^2	candela/m^2	0.2919	foot-Lamberts	fl
FORCE and PRESSURE or STRESS				
N	newtons	0.225	poundforce	lbf
kPa	kilopascals	0.145	poundforce per square inch	lbf/in^2

*SI is the symbol for the International System of Units. Appropriate rounding should be made to comply with Section 4 of ASTM E380.
(Revised March 2003)

Table of Contents

List of Figures

List of Tables

Executive Summary

Bicyclists depend on the visibility of the surrounding environment to maintain a safe travel path. This study used a new method to evaluate pavement marking deterioration for bike lanes. Three paint products were tested: 1) green waterborne paint, 2) green liquid methacrylate (MMA) paint, and 3) white thermoplastic paint. The research team prepared substrates of asphalt mixtures with the paint products for testing. A laboratory, three-wheel polishing device was used to polish (i.e., repeatedly pass over) the test substrates to simulate wear from motorized vehicles and street maintenance equipment. Surface polishing was examined under pneumatic tires, steel wheels, and a steel scraper blade. The pneumatic tires simulated traditional motor vehicle traffic. The steel wheel simulated a more abrasive condition representative of maintenance equipment. In addition, the steel scraper blade was developed and proposed to simulate deterioration of the pavement surface due to snowplowing operations.

The research team measured various characteristics to assess the performance and durability of the pavement marking products. The characteristics were measured after each set of polishing cycles. These performance measures were retroreflectivity, color change, durability, and friction.

Retroreflectivity was measured in dry and wet conditions. Retroreflectivity decreased with the number of polishing cycles. Overall, there was a significant decrease in percentage of retroreflectivity after 1,000 cycles for all testing conditions before retroreflectivity reached a terminal value. These results were consistent with field observations reported in the literature. The steel wheels were found to cause a more significant drop in retroreflectivity for the thermoplastic than the other testing conditions (e.g., the pneumatic tires and scraper blade). The logarithmic model was found to describe the change in the retroreflectivity versus the number of loading cycles with high R^2 values for all the retroreflectivity data sets.

The MMA paint experienced the lowest color loss even after 100,000 cycles, irrespective of the exposure and the testing conditions. It is believed that the small reduction in color was due to the presence of specific chemicals, coupled with thicker paint of the MMA materials in comparison to the thickness of the waterborne materials. The durability results demonstrated that the waterborne markings peeled off the surface with increasing numbers of polishing cycles, unlike the MMA materials, which were polished and washed but did not peel off the surface. The MMA materials endured more three-wheel polisher device loadings than the waterborne

materials under the pneumatic and scraper plate wheelsets. However, there was no significant difference under the steel wheels. The friction results demonstrated that that the MMA surfaces had the highest friction, whereas the thermoplastic had the lowest friction.

On the basis of the results of this study, the laboratory evaluation procedure can be standardized and used as a pre-qualifying test for assessing different pavement marking products or for selecting a suitable material from a set of alternatives for a specific climate or operational conditions. This method reduces the testing time from years (based on field observations) to days (if conducted in the laboratory).

CHAPTER 1. Introduction

1.1. Research Goal

Bicyclists depend on the visibility of the surrounding environment to maintain a safe road path. Therefore, utilizing ideas/techniques that might improve visibility in this environment will have a positive impact on bicyclists' safety. Throughout the country new types of bicycle infrastructure and pavement markings are being installed, such as bike boxes, separated bike lanes, and sharrows. These innovations are intended to improve safety for the growing number of cyclists. One recent innovation is the use of green conflict paint to improve bike lane visibility. In this study, a laboratory-based methodology was implemented to evaluate the performance of various materials used for green conflict paint. Despite the increasing demand for bike lane materials, the durability and long-term weatherability of these products are still unknown. Therefore, evaluation procedures should be implemented to understand the performance of all available materials and to prioritize them to be used in a suitable location and climate.

The goal of is this project was to evaluate the performance of green conflict paint under different simulated deterioration and operating conditions, including rain and snow. The relevant PacTrans theme was Improved Reliability across Modes: decision support tools for winter road maintenance and performance under extreme conditions.

1.2. Research Approach

Three different marking materials (waterborne, green liquid methacrylate [MMA], and white thermoplastic) were evaluated in this study, including green under varying loading conditions. We measured various characteristics, including the following:

1. Friction – using a circular friction device
2. Texture depth – using a sand patch test
3. Daytime color – using a 45/0 geometry chromatic device
4. Nighttime color – using a 30-m geometry chromatic device
5. Luminance – using an ASTM 2073 device
6. Durability and percentage of loss – using high-resolution image analysis
7. Retroreflectivity – using a MX30 retro-reflectometer.

We used a three-wheel polisher device (TWPD) to apply accelerated loading and to polish the painted substrates up to 100,000 cycles. The painted substrates were exposed to different accelerated loading conditions (pneumatic tires, steel wheels, and a steel scraper blade) to simulate and evaluate the deterioration of pavement markings in the field. The evaluated characteristics were measures at different numbers of loading cycles.

1.3. Organization of Report

Chapter 2 provides background about bike lane coloring. Chapter 3 describes the testing materials and methods used for this study. The results are presented in Chapter 4, and Chapter 5 provides concluding remarks.

CHAPTER 2. Background

2.1. Bike Lanes

Bike lanes are part of a roadway adjacent to the car's travel lane that should be occupied only by bicyclists. Bike lanes are commonly installed on the right side of the roadway and are defined by longitudinal pavement markings to show their area boundaries and to direct bicyclists in the right direction. Bike lanes may be entirely colored with bright colors to increase safety. Recently, colored bike facilities have been used to establish order in the roadway and enhance road safety by providing a specific area for bicyclists that will minimize conflict with cars as much as possible. Figure 2.1 shows a green lane installed.

Figure 2.1. Green conflict paint used to enhance bike lane visibility (NACTO, 2012).

The Manual on Uniform Traffic Control Devices (MUTCD) provides guidance on longitudinal markings, arrows, and symbols used along bike lanes, but it does not include guidance for green conflict paint; however, interim approval has been granted for a trial basis (USDOT, 2011). The MUTCD is awaiting research related to material (water-based versus thermoplastic), design (pattern), chromaticity (color specification), and retroreflectivity specifications.

The performance of some pavement markings can degrade significantly after a short period of service. New pavement markings may even have unknown performance until they have been used on roads. Therefore, many cities are evaluating proper material types and patterns to ensure adequate performance and safe operations. For example, the NACTO Urban Bikeway Design Guide offers three suggestions for the pattern of green conflict paint at intersections where right turn pockets are present. Figure 2.2 shows the three suggested designs. Design A (top) specifies solid green paint for the conflict zone. Design B is the opposite application (i.e., green paint in the bike lane but not in the conflict zone). Design C uses dashed green paint for the conflict zone and solid green before the stop bar.

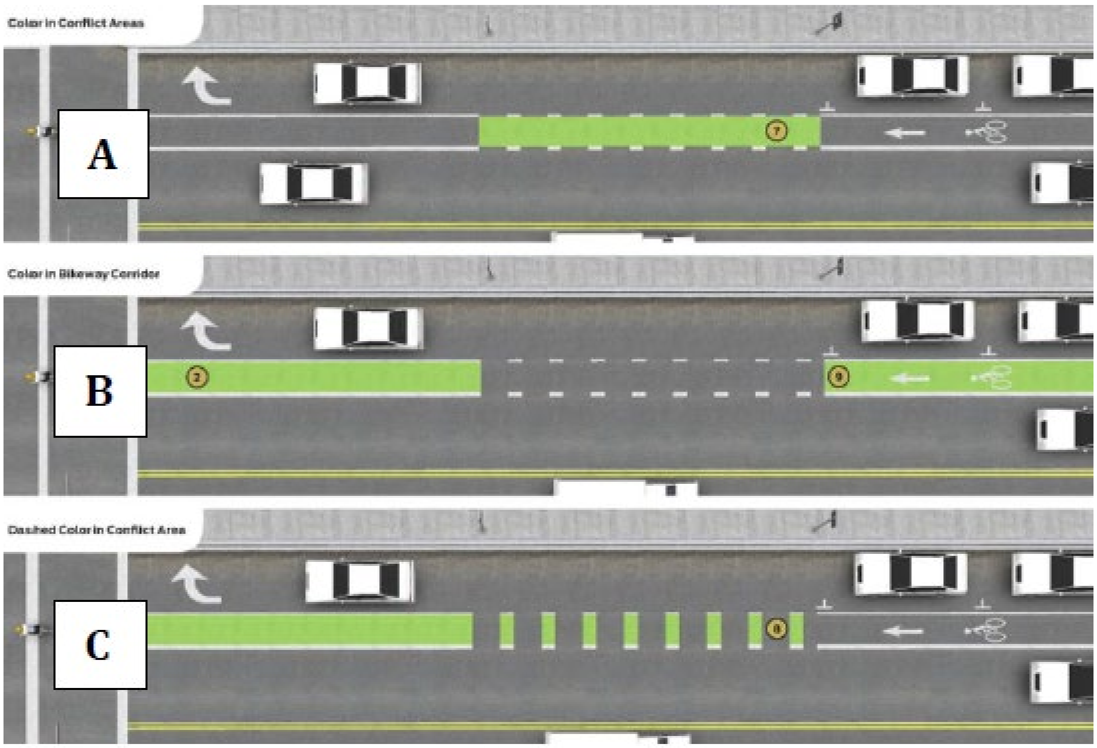

Figure 2.2. Three design alternatives for conflict zones at right turn pockets (NACTO, 2012).

Research is needed to examine various aspects of green conflict paint, including its durability and optimal performance. Some cities have chosen to use Design C on the assumption that dashes are more visible to motorists and because it is less expensive. Research is needed to verify whether dashes have the added benefit of providing better friction for motorists and bicyclists. If this is true, then perhaps solid paint should not be used near the stop bar or at any location where bicyclists are expected to stop suddenly. Friction should be tested under varying degrees of deterioration, weather conditions, and paint materials. The MUTCD's interim approval includes recommendations for daytime and nighttime chromaticity. However, because green paint is new to traffic engineering, it is not clear how the colored paint under the specification will withstand deterioration. Perhaps other color specifications will maintain color better. The MUTCD interim approval does not specify retroreflectivity requirements. Because green paint is new, research is needed to ascertain the characteristics of retroreflectivity under deterioration.

Transportation planners seek to utilize the best available sustainable solutions (e.g., techniques/ideas) to enhance transportation safety. Bicycling is conceded to be an active (e.g., human-powered mode) and sustainable transportation mode. It is one of the health-promoting physical activities that should be encouraged on roads. In most American cities, bicyclists use bike lanes to be safe from conflicts with other transportation modes such as cars and pedestrians. The Federal Highway Administration (FHWA) considers bike lanes to be one of the facilities that encourage bicycling. Even though bike lane facilities serve the same purpose, they are of different types. Generally, bike lanes can be classified into three types on the basis of their location on the street and how they are separated from traffic. They may be completely separated from traffic, adjacent to traffic, or shared with traffic.

2.2. Bike Lane Coloring

One of the rapidly evolving techniques that can be applied to all bike lane types is coloring. All bike lanes types can be improved by "coloring" their paths instead of, or in addition to, designating them by longitudinal pavement markings to differentiate them from other lanes. Because colored bike lanes are one of the newest techniques to increase transportation safety, more research is needed to prove their effectiveness. On the other hand, they may be supported by the fact that coloring the pavement of the bike lane increases its visibility in daytime and nighttime, which in turn will have a positive impact on bicycling safety. Colored bike lanes will also help to identify potential conflict areas and give the right of way to bicyclists in those conflict areas. Bike lanes may be entirely or partially colored. Traffic engineers/practitioners can assess the situation and suggest which part should be colored. This part could be the entire path or only a bike box, conflict area, or intersection crossing marking (NACTO, 2012; FHWA, 2015; Tumlin, 2012; MacNaughton et al., 2014; Koetsier, 2016).

Since the 1990s, colored bike lanes have been implemented by many cities in the United States. Several colors have been used to color bike lane corridors. Some of these colors have had other uses. For example, blue was used in Portland City, although the color blue was intended for parking spaces for people with special needs (Hales et al., 1999). Therefore, it was recommended that colors be used for bike lanes that are not used or described in the MUTCD for other purposes. On that basis, the FHWA approved interim experiments with green in many cities across the United States. Colors such as white, yellow, red, blue, and purple have been clearly identified in the MUTCD for different purposes. Therefore, green is a favorable color for painting bike lanes to reduce confusion with other standard pavement marking colors (MUTCD, 2009; Hunter, 2008).

Generally, pavement markings can be longitudinal, transverse, or temporary. All pavement markings installed crosswise on top of the pavement, from side-to-side, or perpendicular to the road centerline are called transverse pavement markings. Based on the MUTCD, the term "transverse marking" also covers all word and symbol markings, shoulder markings, stop line markings, crosswalk markings, speed measurement markings, parking markings, and transverse median markings. The colors used for common transverse pavement markings are white and yellow, while blue and red colors are permitted under certain conditions (Moser et al., 2015). The unique configurations and designs of transverse pavement markings make them instantly recognized and understood by roadway users (Wang, 2010). Green bike lane markings are considered to be transverse pavement markings because bikes pass directly over them and they are colored from side-to-side along the traffic lanes. White longitudinal pavement markings should be delineated along the edges of the green pavement to be consistent with other marking facilities.

2.3. Green Bike Lane Materials

Pavement marking materials consist of three main ingredients: binder, pigment, and retroreflective material. Binder is the element that helps to keep all the materials together in one structure and glue them to the asphalt/concrete surface texture, while the pigment and the retroreflective material provide the color and enhance the visibility of the pavement markings (Wang, 2010). Numerous types of pavement marking materials are currently used in the highway industry of the United States. Pavement marking materials are classified as either nondurable or durable materials. Durable materials often have an expected service life of more than one year, and nondurable markings have a service life of less (Craig et al., 2007; Schalkwyk 2010; Migletz et al. 2001). The green color may be implemented in two ways: it may be painted on the top of the pavement surface or embedded within the pavement structure (mixed into the pavement) (NACTO, 2012).

Colored pavement markings used for bike lanes may take the form of an overlay (when colors are painted on top of the pavement surface) or may be embedded (when colors are mixed into the pavement material). The materials used for the overlay technique are described below.

Waterborne markings (which can also be called traffic paint or Latex) often have less than one year of expected service life. Therefore, they are considered nondurable pavement markings. Even though waterborne markings have a shorter service life than other marking materials, they are still extensively used on road facilities because of their lower cost and more eco-friendly characteristics in comparison to other products. Waterborne markings are recommended for use on low-volume roads or for use as an interim pavement marking material because they are easily worn by tires and winter maintenance machinery such as snowplows and often require annual maintenance. Figure 2.3 shows an application of a green bike lane made with a waterborne material.

Figure 2.3. A typical green bike lane (NACTO, 2012).

Thermoplastic markings are the second most widely used material in the United States after waterborne markings. Thermoplastic pavement markings are made of several components, including binder, glass beads, titanium dioxide (TiO_2), and filler such as carbon carbonate. They can be alkyd (a naturally occurring resin) or hydrocarbon (a petroleum-derived resin). Alkyd resists oil, but it is sensitive to heat. Hydrocarbon thermoplastic is relatively more heat stable than alkyd thermoplastic. Originally, thermoplastic materials were initially in a granular or block form. The solid-state is changed to liquid by increasing its temperature to more than 204 ºC (400

°F), and the material is then sprayed, extruded, or screed on the top of the pavement surface or melted in place as preformed thermoplastic. That is usually supplied in large pieces to the site and can be used as a longitudinal rumble strip, transverse markings, and marking symbols. Both forms are heated on site to provide adhesion with the pavement surface (Carlson et al., 2013; Wang, 2010). In general, thermoplastic pavement markings adhere well to asphalt pavement, but they can prematurely lose their adhesion with concrete pavement. Therefore, sealers are required before the installation of the thermoplastic markings on concrete pavements to ensure an appropriate bond to the concrete surface (Schalkwyk, 2010). The application of thermoplastic in cold regions is limited because of the poor bond between the material and pavement surfaces at low temperatures. Thermoplastic material formulation, appropriate surface cleaning, moisture removal, and priming before installation (if needed) are factors that should be considered for successful thermoplastic application and performance on concrete pavements (Jiang, 2008a). Anti-skid elements can be applied or mixed throughout the plastic compound (NACTO, 2012).

Epoxy is produced on-site by mixing two materials. Part A (base) includes resin, pigment, extenders, and fillers, while part B (hardener) is a catalyst used to speed up the setting time. Glass beads are also intermixed with the first material before application or applied on the stripe while it is still wet. Epoxy paints are highly durable and can be successfully used on both asphalt and concrete pavements because they provide exceptional adhesion to both pavement surfaces. Epoxy pavement markings are modest in cost in comparison to other types of pavement markings and can last up to four years (for longitudinal markings), but they have less attractive color over time when exposed to intense ultraviolet light. The long drying time of the epoxy during installation limits its use under high traffic volumes. Despite this disadvantage, some survey studies have shown that many transportation agencies use epoxy on concrete pavement with high traffic volumes (Jiang, 2008b). Modified epoxy or urethanes have performance properties comparable to those of epoxies. They are considered to be a little more durable than epoxies, have a faster curing time, and have more color stability when exposed to ultraviolet rays (Carlson et al., 2013; Wang, 2010).

Methyl methacrylate (MMA) is considered to be a nonhazardous material because it contains negligible amounts of volatile organic compounds (VOCs). MMA markings often have an expected service life of more than three years. MMA pavement markings can be applied in cold climates and are resistant to oils, anti-freeze, and other chemicals usually found on pavements. MMA material adheres well to both asphalt and concrete surface textures (Timothy et al., 2003; Jiang, 2008b). In addition, MMA can be also skid resistant (NACTO, 2012).

2.4. Material Enhancements

Pigments can be added to asphalt concrete and paved over as a thin layer over the hot asphalt concrete. This technique has been used in the red bike lanes of Portland, Oregon (NACTO, 2012). NACTO has reported that several cities in the United States have installed green bike lanes by utilizing the pigmented pavement technique. NACTO (2012) has discussed some of the advantages and disadvantages. Installing this kind of colored pavement requires the additional steps of applying a primer (Koetsier, 2016).

The term retroreflectivity describes how light that originates from vehicle headlights illuminates the visible pavement marking surface and then returns back to the driver's eye. These retroreflected light rays assist roadway users in dark conditions with significant information related to driving performance and safety, such as the roadway alignment, speed, vehicle lateral position, and other driving-related factors (Parker and Meja 2003). Retroreflectivity is measured in units of millicandelas per square meter per lux (mcd/m2/lux), which is expressed as the coefficient of retroreflected luminance (R_L). In past research, pavement marking retroreflectivity has been extensively used as an important indicator in analyzing pavement marking material performance and cost effectiveness (Zhang and Wu 2010).

Because only a small portion of light is retro-reflected to the driver’s eyes from the pavement marking, installing glass beads is a widely used practice to increase the amount of reflected light, which in turn increases the visibility of the pavement markings. Glass beads are small globular glass balls that are used to improve the retroreflectivity of pavement marking material. Coating the glass bead surface (treated glass beads) allows them to sink into the paint to provide continuous retroreflectivity while the paint is wearing. Glass beads can be intermixed with the binding material before application or during application of the pavement markings by dropping them on the top of the painted marking material while the marking is wet (Jiang 2008b). Five types of glass beads (I, II, III, IV, and V) have been classified by the American Association of State Highway and Transportation Officials (AASHTO) under the Standard Specification for Glass Beads Used in Pavement Markings (AASHTO M 247). Type I is known as the standard bead or standard gradation, while types II, III, IV, and V have respectively larger bead gradations and are known as modified gradations.

Digital cameras and retro-reflectometers have been used to collect field or laboratory data related to glass bead studies. Bead density is then calculated directly from photos. Nowadays, computer software is used to ease the task of counting glass beads in high resolution pictures (Migletz and Graham 2002a; Zhang et al. 20010). For example, NCHRP Report 743 used glass bead quality as an indicator for predicting the initial retroreflectivity of pavement markings by using high-resolution cameras and retro-reflectometers in the field and in the laboratory. In the same research, a draw-down test procedure was developed in the laboratory for measuring enough samples of pavement markings with different characteristics. In this laboratory procedure, controlled thicknesses of pavement markings were painted on flat objects, and glass beads were dropped on the top of the wet markings in a consistent manner to be evaluated later (Smadi 2013).

2.5. Pavement Marking Cost

Departments of transportation (DOTs) consider pavement markings to be one of the most effective low-cost devices for improving highway safety (Miles et al. 2010). Each pavement marking material has its own unique installation method, lane closure duration, and service life. Consequently, each material has a different cost. Reducing cost by selecting a suitable pavement marking material that meets specifications is of great interest to state DOTs. Therefore, a cost-benefit analysis should be implemented to determine how well, and how poorly, each option performs. Several factors are considered when a pavement marking material is selected, such as climate, service life (durability), and cost. When calculating cost, it is important to consider not only the material cost but also the cost of the crew and the installation equipment necessary. In addition, the life-cycle cost of a pavement marking material is directly affected by its durability and its ability to resist surrounding effects. In other words, marking materials that have a short lifespan need to be restriped more frequently (Gibbons et al. 2013). Also, retroreflectivity has been used broadly in previous studies as a significant factor in analyzing the cost effectiveness of the marking material.

The NACTO guide provided the cost of several pavement marking materials. Table 2.1 shows the material prices per square foot and expected performance.

Table 2.1. Material prices per square foot and expected performance (NACTO, 2012).

Type of Material	Prices per square foot and expected performance
Non-durable waterborne paint	$0.60 sq. ft. for raw materials, $1.20 - $1.60 sq. ft. installed. Could last ½ year to 2 years based on weather
Epoxy-based durable liquid pavement markings (DLPM)	Sunlight and water may reduce color intensity
Epoxy pavement marking	$1.00 - $3.00 sq. ft. for raw materials. $8.00 - $11.00 sq. ft. to install, with skid resistance and longevity as long as 3 – 5 years
Methyl methacrylate (MMA)	$3.00 - $4.00 sq. ft. for raw materials. $8.00 - $11.00 sq. ft. to install, and may last as long as 3 – 6 years
Thermoplastics	$3.00 - $6.00 sq. ft. for raw materials. $10.00 - $14.00 sq. ft. to install, wears well in conflict areas and spot fixes
Embedded (colored asphalt)	Pigmented asphalt costs are between 30 to 50 percent more than conventional asphalt, a layer at least 1 cm thick is expected to last for the life of the pavement

CHAPTER 3. Test Materials and Methods

3.1. Test Materials

The research team prepared test substrates made of asphalt mixtures. The asphalt mixture was a dense graded mix used at a paving project in the state of Idaho. The research team collected loose materials from the field and prepared the slabs in the laboratory. The asphalt mixture was made of basalt aggregates and PG 64-34 asphalt binder (5.5 percent by weight). The asphalt mixture was placed in a steel mold and compacted with a plate compactor (see figure 3.1a-c). Afterwards, some prepared slabs were transported for painting at the Idaho Transportation Department (ITD) in Lewiston, Idaho, and left for 48 hours before testing. A total number of nine asphalt slabs were prepared. The size of the test slabs was 20 in x 20 in x 4 in. Three replicates from each pavement bike lane material were prepared and tested.

The asphalt substrates were painted with three different paints and tested under different operating conditions (pneumatic tire, steel wheel, and steel scraper blade) (table 3.1). The steel wheel caused more deterioration to the pavement surface than the pneumatic tire. The steel scraper blade was developed and proposed to simulate deterioration of the pavement surface due to snowplowing operations (Mohamed et al. 2020). To simulate snowplowing in the laboratory experiment, a scraper steel blade was installed in between the pneumatic wheels of the TWPD's turntables. The paints used in this study were (i) green waterborne paint, (ii) green liquid methacrylate (MMA) paint, and (iii) white thermoplastic paint, as shown in figure 3.1d-f. For the green waterborne paint, a bead-dropping rate for the green waterborne paint (glass bead dosage) of 0.95 kg/L was spread on half of the slab surface to evaluate the loss of paint's reflectivity, as shown in figure 3.1d-f. The performance of the new green liquid methacrylate paint was investigated and compared to that of the green waterborne paint. The paint was prepared by mixing a certain quantity of glass beads according to the manufacturer's specifications, and then it was spread on the slab surface.

The third paint utilized in this study was a melt-in-place, preformed thermoplastic pavement marking (alkyd formulation). It was purchased and supplied to the site as a solid segment and then fused to the slab surface (after preheating of the slab), with a propane torch as the source of heat (figure 3.1g). However, unlike the other green paint employed, no additional glass beads were added on the surface because the preformed thermoplastic was premixed with required glass beads. An additional slab was prepared for friction testing for the waterborne paint without glass beads.

Table 3.12: Paint types and testing conditions included in the study

Paint types	**Testing conditions**		
	Pneumatic tire	Steel plate	Steel scraper blade
Waterborne paint	x	x	x
White thermoplastic paint	x	x	x
Green liquid methacrylate (MMA) paint	x	x	x

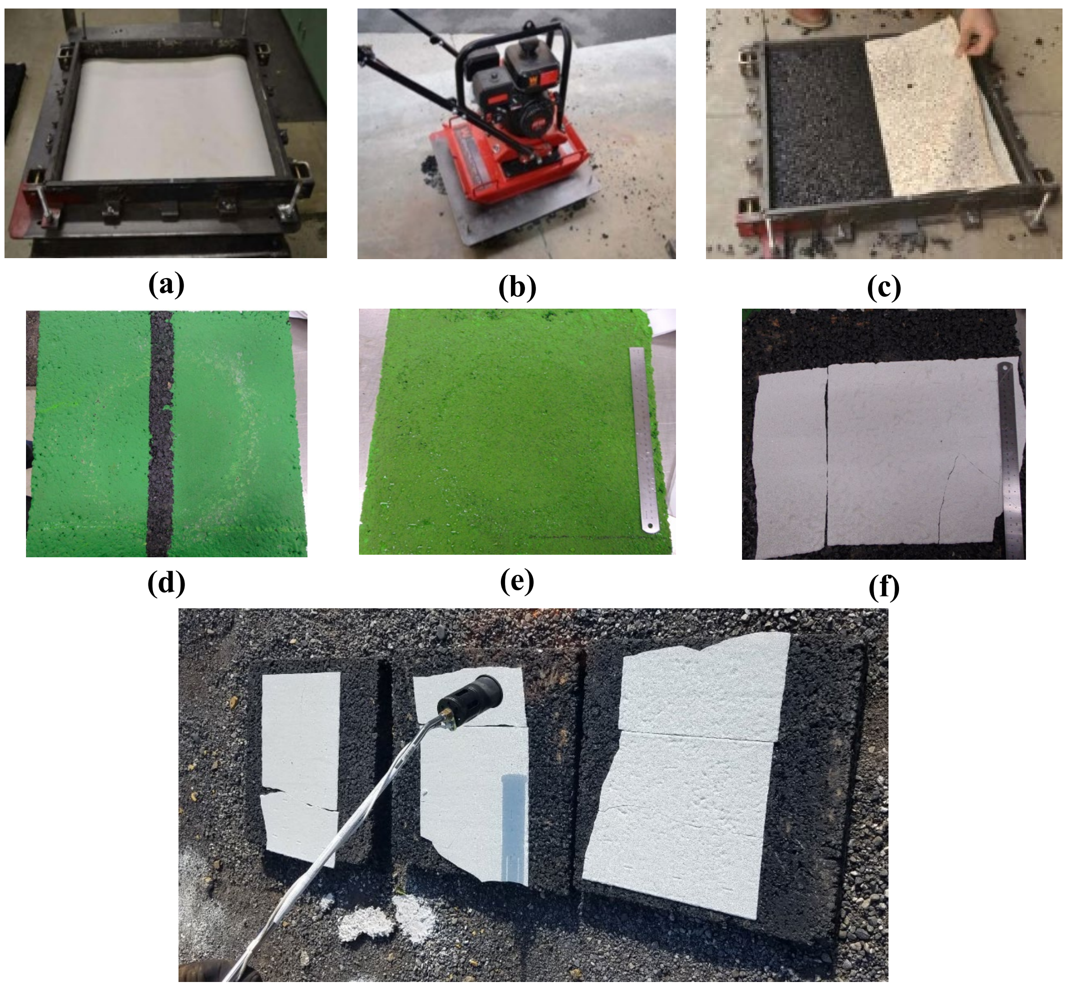

(a) **(b)** **(c)** **(d)** **(e)** **(f)** **(g)**

Figure 3.1. Sample preparation procedure (a) square steel mold; (b) plate compactor machine; (c) asphalt substrates after casting; (d – f) sample painting with green waterborne paint, green liquid methacrylate (MMA) paint, and white thermoplastic paint, respectively; (g) fusion of thermoplastic into the slab using a propane torch as the source of heat.

3.2. Accelerated Traffic and Climatic Loading Conditions

Each of the painted substrates was exposed to different accelerated loading conditions (pneumatic tire, steel wheel, and steel scraper blade) to simulate and evaluate the deterioration of pavement markings in the field. A three-wheel polisher device (TWPD) was used to apply accelerated loading and to polish the painted substrates up to 100,000 cycles (figure 3.2a). The TWPD had three pneumatic rubber tires mounted on a turn table that was 11 in. in diameter. The wheel cluster with an applied load rotated on the slab to simulate polishing by traffic in the field. The test was conducted in the presence of water to wash away any fine materials resulting from the polishing. After a set of polishing cycles, several characteristics were measured, including durability, retroreflectivity, color changes, and friction of the test materials. The retroreflectivity was measured in dry and wet conditions. The testing matrix for this study is summarized in table 3.1.

Table 3.1. Testing matrix for the pavement marking deterioration

Testing procedure	**Testing Device**	**No of cycles**	**Wheelset**	**Paint type**		
				Waterborne	**MMA**	**Thermoplastic**
Accelerated loading testing	Three-wheel polisher device (TWPD)	0, 100, 1000, 10000, 50000, and 10000	Pneumatic tires; Steel wheels; Scraper blade	$R_{L,1,2}$; C ; D; F	$R_{L,1,2}$; C ; D; F	$R_{L,1,2}$; C ; D; F

where $R_{L,1,2}$ is the retroreflectivity in dry and wet conditions; C is the surface colors change; D is the durability characteristics, and F is the coefficient of friction

3.3. Performance Measures

The research team measured various characteristics to assess the performance and durability of the test bike lane pavement markings. Four major performance measures were assessed at different numbers of polishing cycles to investigate the deterioration of pavement markings. These performance measures included retroreflectivity, surface color change, durability, and change in surface friction.

3.3.1. Retroreflectivity

Using an Mx30 reflectometer, the retroreflectivity in dry (R_L) [in accordance with ASTM E1710 (ASTM 2018a)], recovery (R_{L1}) [ASTM E2177 standards (ASTM 2018b)], and continuous wetting (R_{L2}) [ASTM E2176 standards (ASTM 2008)] conditions were measured. A typical reflectometer used in this study is shown in figure 3.1b. Multiple readings were taken on the substrate surface to account for measurement variability, which were then averaged. The standard unit of retroreflectivity is $mcd/m^2/lx$ or mcd.

The MX30 retro-reflectometer can capture a dimensional area of up to 4 in x 3.5 in (10 x 9 cm) approximately, while the wheel path from the tire covers a smaller area of only 1.6 in x 3.2 in (4 x 8cm); therefore, a correction was needed. To accommodate these differences, retroreflectivity measurements were taken consistently with a frame area of 1.6 in x 3.2 in and then multiplied by an adjustment factor. A similar adjustment was also carried out for both the steel wheel and the scraper blade.

3.3.2. Surface Colors Change

The color surface deterioration was measured by using the high-quality NR200 calorimeter. The calorimeter was made of a 0.31-in-diameter aperture following the ASTM D2244 (ASTM 2016a) standards, as shown in figure 3.1d. The total color change (ΔEab) and lightness change (ΔL) were calculated by using Eq. 1 and Eq. 2, following the CIELab 1976 color space.

$$\Delta Eab = (\Delta L^2 + \Delta a^2 + \Delta b^2)^{1/2} \tag{1}$$

$$\Delta L = (\Delta L^2_{Reference} - \Delta L^2_{Sample})^{1/2} \tag{2}$$

where L (lighter or darker), a (yellow-blueishness), and b (red-greenishness) describe the surface characteristics. A positive L value indicated the presence of lighter color, whereas a negative L value indicated a darker color.

3.3.3. Durability

High-resolution digital images were captured for the surface of the test slabs after a set number of polishing cycles (i.e., 0, 100, 1,000, 10,000, 50,000, and 100,000 cycles). The ImageJ software was used to analyze the captured images and calculate the percentage loss of pavement markings. To ensure accurate and consistent readings, the camera was mounted at a constant height in a fluorescent light environment. The ImageJ software processed and analyzed the images to quantify the worn area on the pavement surface where the paint was lost or fading because of loading and polishing. The durability rating methodology was employed to evaluate the remaining paint materials at the surface (i.e., 100 percent indicated no loss, whereas 0 percent indicated complete loss of paint materials at the surface).

3.3.4. Surface Friction

In this study, the friction characteristics of painted test slabs were evaluated by measuring the mean texture depth (MTD) and the coefficient of friction by using the volumetric sand patch test and dynamic friction tester, respectively. The sand patch test was conducted in accordance with ASTM E 965. The surface of the painted test slabs was cleaned with a brush and then a known volume of silica sand was spread over the test surface in a circular pattern. The diameter of the circular patch was measured, and the MTD was calculated by using Eq. 3.

$$MTD = 4V/(\pi D^2) \quad (3)$$

where, MTD = mean texture depth (mm), V = sand volume (mm^3), and D = average diameter of sand patch circle (mm)

The coefficient of friction was measured by using the dynamic friction tester (DFT) in accordance with ASTM E1911. The DFT is a portable device that can be used in the field and laboratory. The DFT consisted of three rubber sliders attached to a rotating circular disk, as shown figure 3.1f and 3.1g. The circular disk rotated at a desired testing speed (up to 100 km/h). The disk was then dropped so that the rubber sliders were in contact with the pavement surface. The coefficient of friction was measured as the speed of the rotating disk gradually decreased (Saito et al. 1996; Beautru et al. 2011; Aldagari et al. 2018). The coefficient of friction at 20 km/hr (DFT20) was used as an indirect method to measure pavement micro texture (Beautru et al. 2011; Kane et al. 2015). Figure 3.1h shows the interface of the DFT software. After a number of friction tests and depending on the level of surface friction, the rubber sliders were replaced periodically.

Skid resistance can be quantified by calculating the international friction index (IFI). In this study, the IFI was calculated by using the MTD and DFT20 measured with the sand patch test and DFT, respectively, in accordance with ASTM E 2157 and the Pavement International Association of Road Congress (PIARC) formula, as given in Eq. 4 to Eq. 6.

$$IFI = 0.081+0.732\ DFT_{20}\ \exp(-40/S_p) \quad (4)$$

$$S_p = 14.2+89.7\ MPD \quad (5)$$

$$MTD = 0.947\ MPD +0.069 \quad (6)$$

where, DFT_{20} = coefficient of friction at 20 km/h measured with DFT; S_p = speed constant; MPD = mean profile depth; MTD = mean texture depth

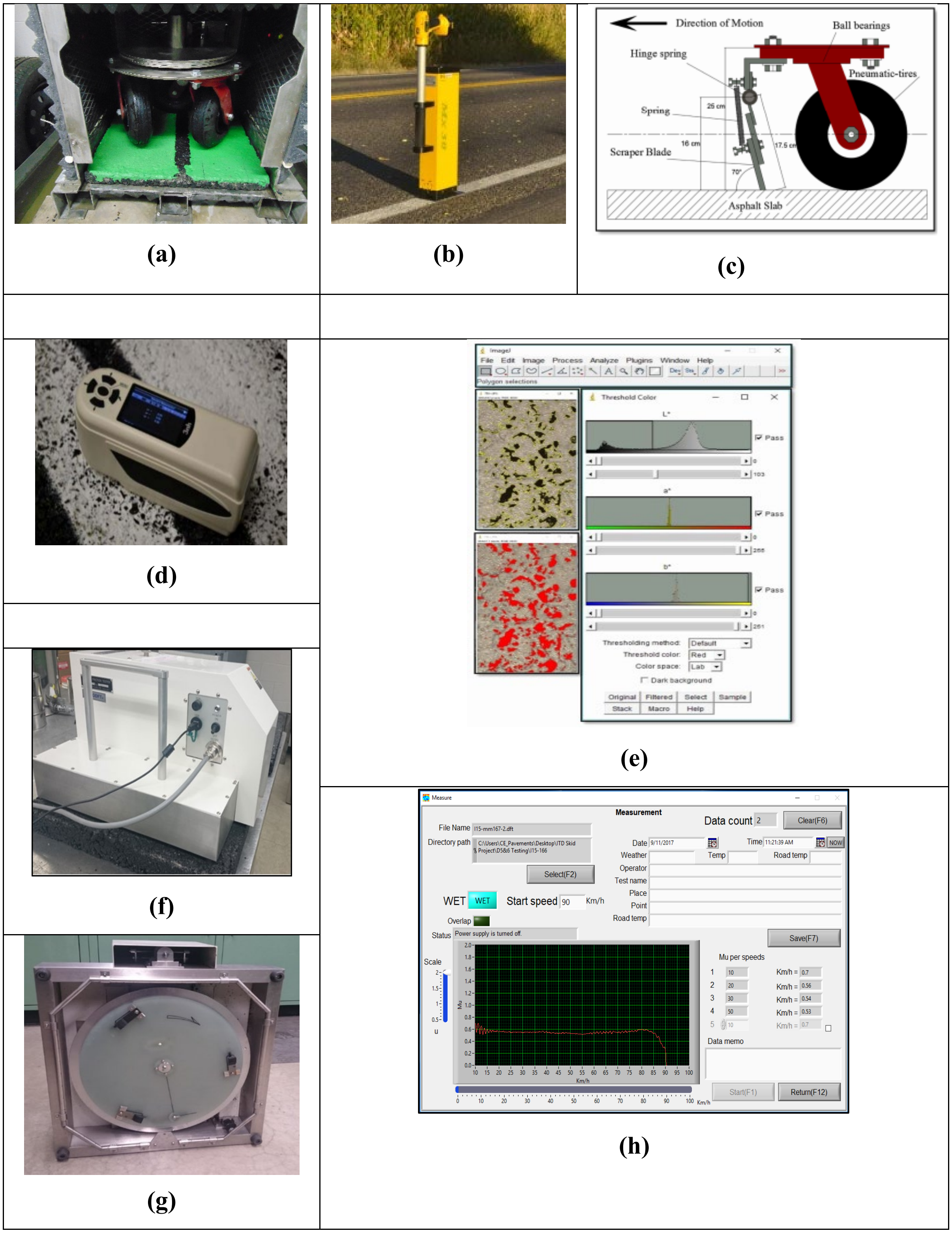

Figure 3.2. (a) TWPD wheelset set-up; (b) MX 30 retro-reflectometer; (c) Snowplow loading simulation; (d) Colorimeter; (e) ImageJ software interface (f) DFT device; (g) Bottom of the DFT with three rubber sliders; (h) Coefficient of friction measurements by DFT software

CHAPTER 4. Results

4.1. Retroreflectivity Deterioration

The laboratory measurements collected on retroreflectivity were analyzed to investigate the deterioration of the test pavement markings. The retroreflectivity of the three pavement marking types (i.e., waterborne, MME, and thermoplastic) were measured in both dry and wet conditions with a number of polishing cycles. In addition, the retroreflectivity characteristics were investigated under three different polishing operating conditions (i.e., pneumatic tires, steel wheels, and scraper blade installed with pneumatic tires). The retroreflectivity was measured at various spots along the polished wheel path, and the average was calculated. In general, there was a significant decrease in percentage of retroreflectivity after 1,000 cycles for all testing conditions before a terminal value was reached with a number of cycles. The percentage of retroreflectivity for each loading condition was evaluated and plotted against the number of cycles for the three pavement markings, as shown figure 4.1 to figure 4.4. Table 4.1 summarizes the percentage of retroreflectivity after different polishing cycles and testing conditions. Likewise, equations and the coefficient of determination (R^2) illustrating the relationship between percentage of retroreflectivity and number of polishing cycles were examined and are summarized in table 4.2.

Figure 4.1 shows the percentage of retroreflectivity (PR) versus number of cycles under each loading wheelset for the thermoplastic pavement marking in wet and dry conditions. As expected, the retroreflectivity for the test samples decreased with the number of cycles. The drop in retroreflectivity was significant from the start to 10,000 cycles, whereas the drop was relatively small between 10,000 to 100,000 cycles, after which the test was terminated. These results were similar to the performance of pavement markings in the field. According to Kopf (2004) and Mohamed et al. (2019), the retroreflectivity of pavement markings drastically decreased immediately after installation, followed by a stable drop until the end of their service life (Kopf, 2004; Mohamed et al., 2019).

The percentage of loss in retroreflectivity (LIR) for the thermoplastic materials tested under the steel wheelset was higher (about 78 percent reduction after 100,000 cycles) than under the pneumatic wheelset (25 percent reduction) or scraper blade set (50 percent reduction). This was due to the harsh polishing conditions caused by the steel wheelset. The steel wheelset severely changed the surface of the test samples even after 10,000 cycles (30 percent reduction after 10,000 cycles). The scraper blade set also caused significant reduction in retroreflectivity (about 50 percent) because of the abrasion caused by the blade. Furthermore, the percentage of loss in retroreflectivity in wet conditions was higher than in dry conditions. For example, the thermoplastic materials experienced a drop of 91 percent in PR under the steel wheelset in wet conditions in comparison to a 78 percent drop in dry conditions. This was also consistent with the findings from Mohamed et al. (2019).

Figure 4.2 shows the PR for the MME materials under different loading conditions in wet and dry conditions. The loss in retroreflectivity for the MME materials followed a trend similar to that of the thermoplastic materials. However, the LIR was generally less than that of the thermoplastic paint, in which, after 100,000 cycles, the LIR was 49 percent for the steel wheelset, 42 percent for the scraper blade set, and 34 percent for the pneumatic wheelset in dry conditions.

Figure 4.3 shows the PR under different loading conditions in wet and dry conditions for the green waterborne paint mixed with glass beads, figure 4.4 shows the results for the green waterborne paint without glass beads. Like thermoplastic and MME materials, retroreflectivity decreased with the loading cycles. In comparing the retroreflectivity performance of the waterborne paint with glass beads to the one without glass beads, overall, the former had a smaller percentage of loss than the latter in both dry and wet conditions. This is could be because the waterborne paint without glass beads had lower retroreflectivity than the waterborne paint with glass beads. Also, note that the green waterborne paint was thinner in comparison to the thermoplastic and MME materials at the surface. A noticeable reduction in thickness was observed for the waterborne paint even after only 1,000 cycles.

The research team examined various models (i.e., linear, logarithmic, exponential, and power) to describe the change in retroreflectivity in relation to the number of loading cycles. Table 4.2 summarizes the evaluated models and associated R^2 values. The results showed that the logarithmic model provided the highest R^2 value for all the retroreflectivity data. Furthermore, the logarithm model could predict the reduction in retroreflectivity even after the first 10,000 cycles. The model for the PR of the test marking materials can be generally represented by the model in Equation 7.

$$y = -m * \ln(x) + r \quad (7)$$

where, y is the predicted retroreflectivity value; m = slope of the model; x is the number of cycles, and r is the initial retroreflectivity value.

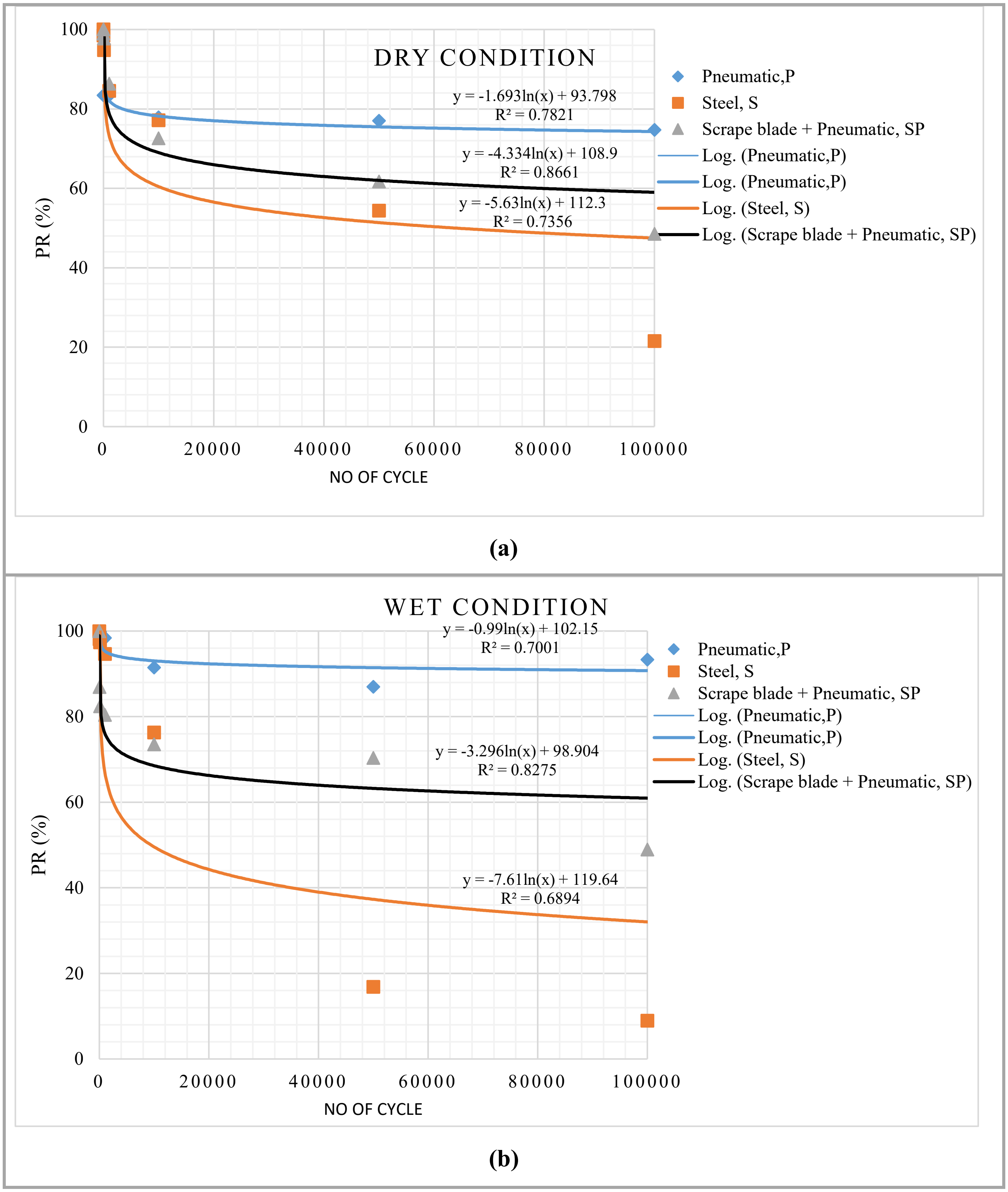

Figure 4.1. A plot of the percentage of retroreflectivity at different loading conditions for thermoplastic materials in (a) dry and (b) wet conditions

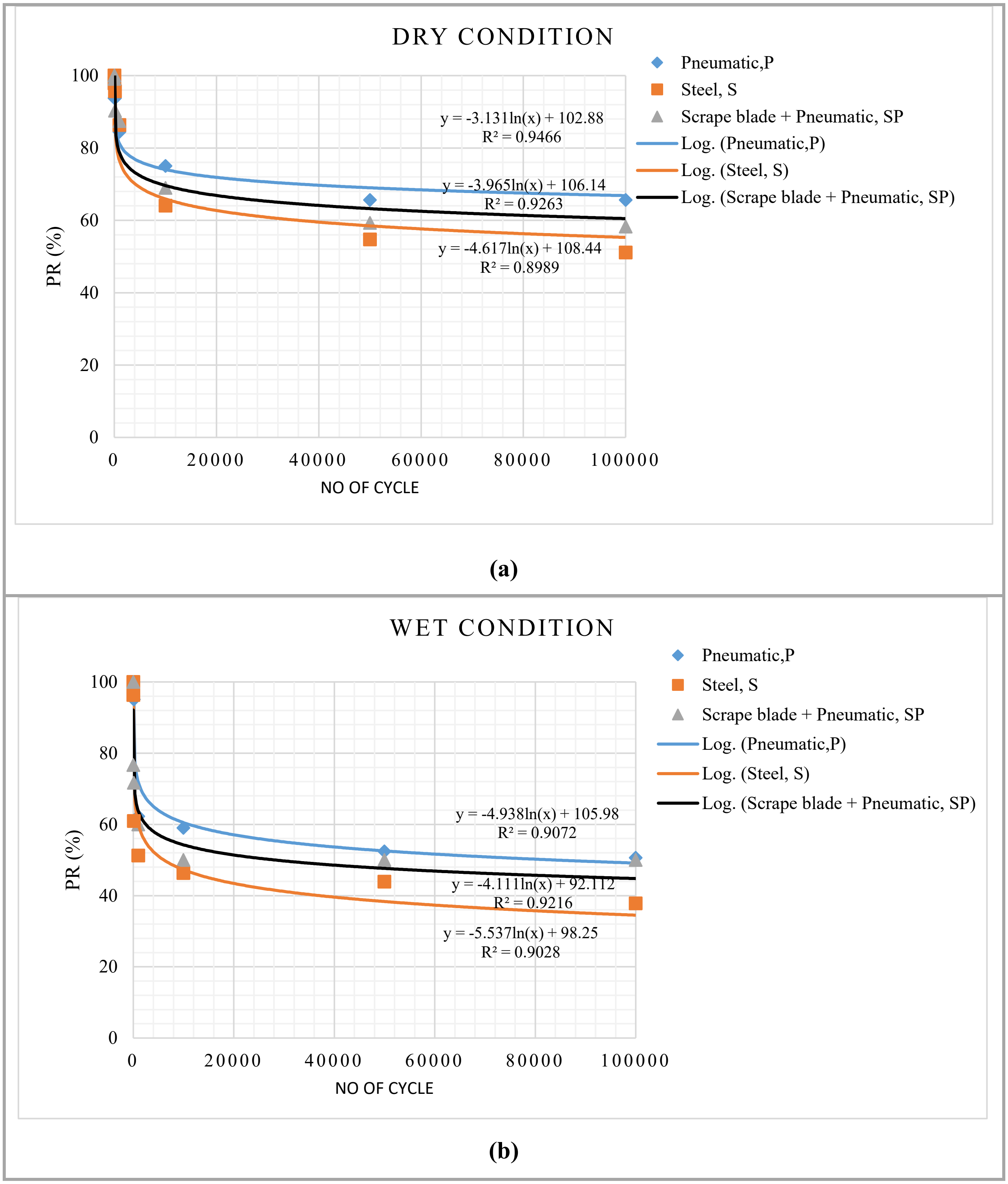

Figure 4.2. A plot of the percentage of retroreflectivity at different loading conditions for MMA materials in (a) dry and (b) wet conditions

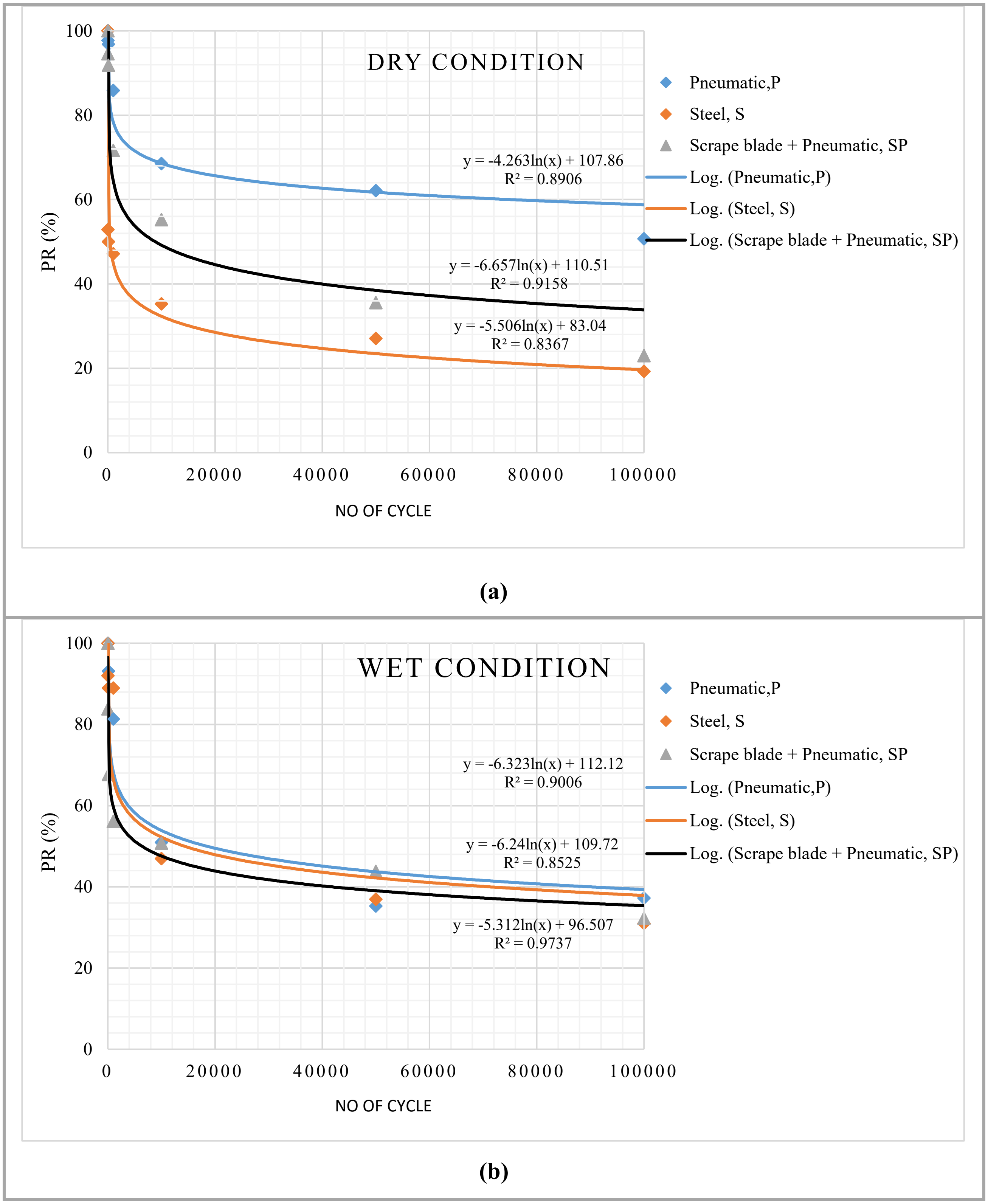

Figure 4.3. A plot of the percentage of retroreflectivity at different loading conditions for waterborne (with glass beads) material in (a) dry conditions and (b) wet conditions

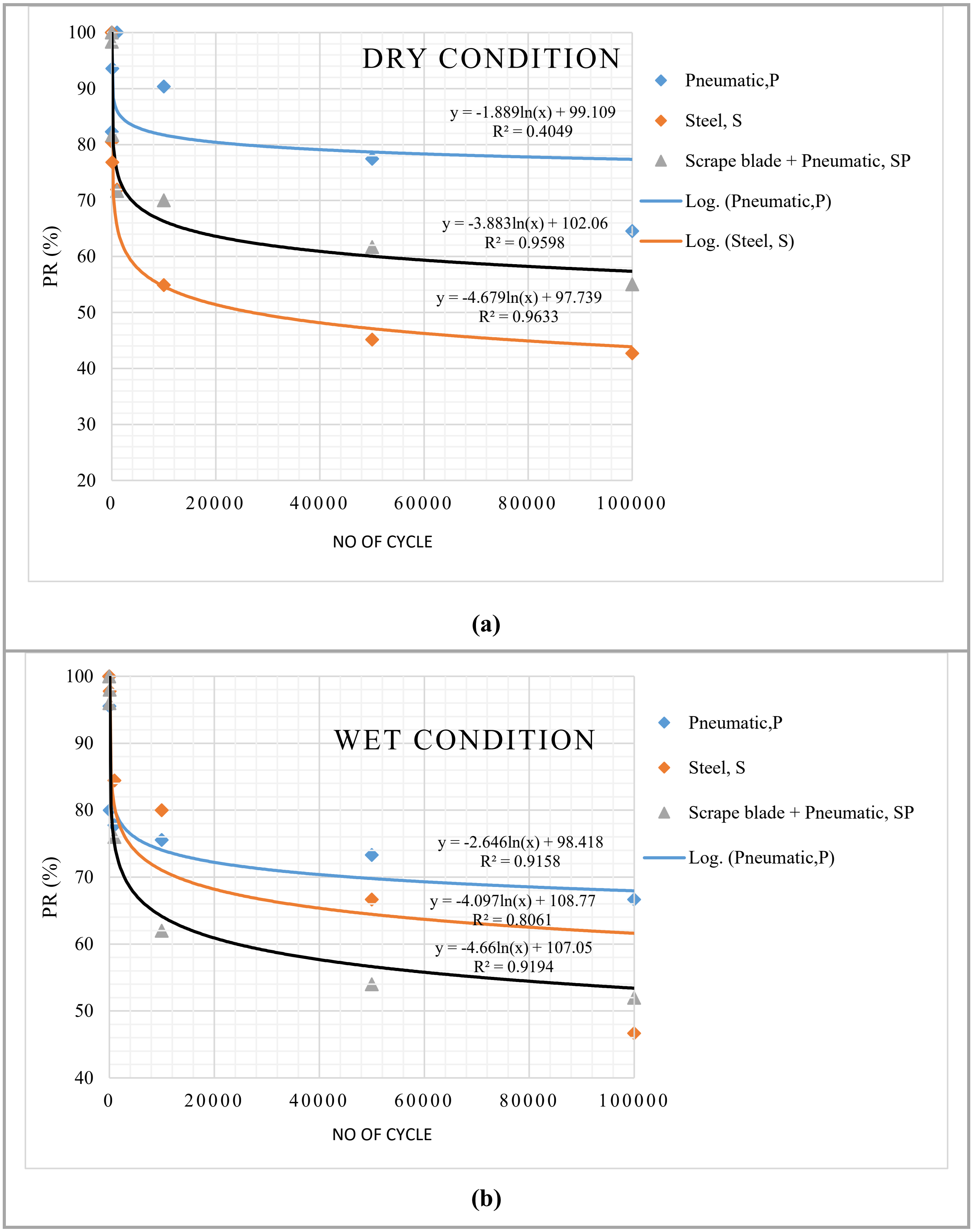

Figure 4.4. A plot of the percentage of retroreflectivity at different loading conditions for waterborne (without glass beads) material in (a) dry conditions and (b) wet conditions.

Table 4.1. Change in percentage of retroreflectivity with number of polishing cycles at different conditions

Retroreflectivity results under dry conditions (%)												
	Thermoplastic material			MME material			Waterborne (with GB)			Waterborne (without GB)		
No of cycle	Pneum-atic	Steel	Scraper blade + Pneumatic	Pneum-atic	Steel	Scraper blade + Pneumatic	Pneum-atic	Steel	Scrape blade + Pneumatic	Pneum-atic	Steel	Scraper blade + Pneumatic
1	100	100	100	100	100	100	100	100	100	100	100	100
10	83	98	99	94	98	99	53	95	98	98	80	82
100	83	95	98	94	96	90	50	92	97	82	77	94
1000	83	85	86	84	86	87	47	72	86	72	72	100
10000	78	77	73	75	64	69	35	55	68	70	55	90
50000	77	54	62	66	55	59	27	36	62	62	45	77
10000 0	75	22	48	66	51	58	19	23	51	55	43	65
Retroreflectivity results under wet conditions (%)												
No of cycle	Thermoplastic material			MME material			Waterborne (with GB)			Waterborne (without GB)		
	Pneum-atic	Steel	Scraper blade + Pneumatic	Pneum-atic	Steel	Scraper blade + Pneumatic	Pneum-atic	Steel	Scrape blade + Pneumatic	Pneum-atic	Steel	Scraper blade + Pneumatic
1	100	100	100	100	100	100	100	100	100	100	100	100
10	100	98	87	98	96	77	100	92	84	96	96	100
100	100	97	82	95	61	72	93	89	68	98	80	98
1000	98	95	80	62	51	60	81	89	56	76	78	84
10000	92	76	74	59	46	50	51	47	51	62	76	80
50000	87	17	70	52	44	50	35	37	44	54	73	67
100000	93	9	49	51	38	50	37	31	32	52	67	47

Table 4.2: Different models to describe the relationship between the retroreflectivity value and number of cycles

Materials	Conditions	Relationship model	Pneumatic, P		Steel wheel, S		Scrape blade + pneumatic (Sb + P)	
			Model	R-squared	Model	R-squared	Model	R-squared
Thermoplastic	Dry condition	Linear	y = -0.0001x + 85.811	0.3553	y = -0.0007x + 92.59	0.9551	y = -0.0005x + 91.849	0.8208
		Logarithmic	y = -1.693ln(x) + 93.798	0.7821	y = -5.63ln(x) + 112.3	0.7356	-4.334ln(x) + 108.9	0.8661
		Exponential	y = 85.516e-2E-06x	0.3939	y = 94.992e-1E-05x	0.9749	y = 91.637e-7E-06x	0.8864
		Power	y = 93.745x-0.02	0.808	y = 127.54x-0.096	0.5748	y = 113.65x-0.057	0.8131
	Wet condition	Linear	y = -8E-05x + 97.592	0.3593	y = -0.001x + 92.911	0.8878	y = -0.0004x + 85.951	0.7873
		Logarithmic	y = -0.99ln(x) + 102.15	0.7001	y = -7.61ln(x) + 119.64	0.6894	y = -3.296ln(x) + 98.904	0.8275
		Exponential	y = 97.5e-8E-07x	0.3518	y = 94.008e-3E-05x	0.9595	y = 86.037e-5E-06x	0.8541
		Power	y = 102.31x-0.01	0.6884	y = 165.81x-0.179	0.6012	y = 101.35x-0.044	0.748
MMA	Dry condition	Linear	y = -0.0003x + 89.364	0.6482	y = -0.0005x + 89.057	0.6848	y = -0.0004x + 89.21	0.6622
		Logarithmic	y = -3.131ln(x) + 102.88	0.9466	y = -4.617ln(x) + 108.44	0.8989	y = -3.965ln(x) + 106.14	0.9263
		Exponential	y = 88.882e-4E-06x	0.683	y = 88.018e-6E-06x	0.7364	y = 88.422e-5E-06x	0.7034
		Power	y = 104.62x-0.038	0.9283	y = 113.32x-0.062	0.8733	y = 109.31x-0.051	0.902
	Wet condition	Linear	y = -0.0004x + 83.215	0.464	y = -0.0004x + 71.56	0.3638	y = -0.0003x + 71.897	0.329
		Logarithmic	y = -4.938ln(x) + 105.98	0.9072	y = -5.537ln(x) + 98.25	0.9028	y = -4.111ln(x) + 92.112	0.9216
		Exponential	y = 81.06e-6E-06x	0.5159	y = 68.229e-7E-06x	0.461	y = 69.97e-4E-06x	0.3778
		Power	y = 109.75x-0.067	0.9137	y = 101.39x-0.085	0.9424	y = 93.477x-0.06	0.9554

Table 4.2 (cont.): Different models to describe the relationship between the retroreflectivity value and number of cycles

Materials	Conditions	Relationship model	Pneumatic, P		Steel wheel, S		Scrape blade + pneumatic (Sb + P)	
			Model	R-squared	Model	R-squared	Model	R-squared
Waterborne (with Glass Beads)	Dry condition	Linear	y = -0.0004x + 90.514	0.7573	y = -0.0004x + 57.581	0.4214	y = -0.0007x + 83.284	0.7657
		Logarithmic	y = -4.263ln(x) + 107.86	0.8906	y = -5.506ln(x) + 83.04	0.8367	y = -6.657ln(x) + 110.51	0.9158
		Exponential	y = 90.03e-6E-06x	0.822	y = 54.544e-1E-05x	0.6877	y = 82.449e-1E-05x	0.9009
		Power	y = 112.08x-0.056	0.8514	y = 88.264x-0.115	0.8993	y = 88.264x-0.115	0.8993
	Wet condition	Linear	y = -0.0006x + 85.049	0.6368	y = -0.0006x + 83.892	0.6834	y = -0.0005x + 72.462	0.5434
		Logarithmic	y = -6.323ln(x) + 112.12	0.9006	y = -6.24ln(x) + 109.72	0.8525	y = -5.312ln(x) + 96.507	0.9737
		Exponential	y = 82.293e-1E-05x	0.6919	y = 81.581e-1E-05x	0.7664	y = 70.749e-8E-06x	0.7007
		Power	y = 123.55x-0.098	0.8584	y = 122.3x-0.102	0.8204	y = 101.96x-0.086	0.9527
Waterborne (without Glass Beads)	Dry condition	Linear	y = -0.0003x + 93.748	0.786	y = -0.0004x + 77.02	0.5931	y = -0.0003x + 84.736	0.5713
		Logarithmic	y = -1.889ln(x) + 99.109	0.4049	y = -4.679ln(x) + 97.739	0.9633	y = -3.883ln(x) + 102.06	0.9598
		Exponential	y = 93.711e-4E-06x	0.8278	y = 75.651e-7E-06x	0.6864	y = 83.906e-5E-06x	0.6531
		Power	y = 99.87x-0.023	0.4074	y = 102.19x-0.071	0.9443	y = 104.25x-0.05	0.9535
	Wet condition	Linear	y = -0.0002x + 86.233	0.4712	y = -0.0005x + 93.485	0.8909	y = -0.0004x + 86.629	0.5913
		Logarithmic	y = -2.646ln(x) + 98.418	0.9158	y = -4.097ln(x) + 108.77	0.8061	y = -4.66ln(x) + 107.05	0.9194
		Exponential	y = 85.744e-3E-06x	0.5248	y = 93.767e-7E-06x	0.9408	y = 85.24e-6E-06x	0.648
		Power	y = 98.969x-0.032	0.9226	y = 113.43x-0.054	0.7263	y = 111.38x-0.063	0.9112

4.2. Surface Color Change Analysis

The color difference was used in this research as a performance measure to quantify the effect of different conditions on the original color of the test samples. Figure 4.5 through figure 4.8 show the total color change (ΔE_{ab}) and change in lightness (ΔL) versus number of cycles for the thermoplastic, MMA, and waterborne materials, respectively, under different loading conditions. The ΔL and ΔE_{ab} for all samples tended to follow a logarithmic function similar to that of retroreflectivity. In figure 4.5 through figure 4.8, the zero value in ΔEab and ΔL is the starting color for each material, and the higher the number. the lower the visibility (drop in color) of the sample. For thermoplastic marking materials, no significant changes in ΔE_{ab} and ΔL were observed under the pneumatic wheel in comparison to the scraper blade and steel wheelsets (figure 4.5a and 4.5b). This drop in color was due to the harsh effect of the steel and scraper blade on the pavement marking, which negatively affected the surface color as the number of cycles increased. The steel and the scraper blade wheelsets were more abrasive than the pneumatic wheelsets, which was consistent with the loss of retroreflectivity and previous findings by Mohamed et al. (2019; 2020).

No significant change in color was observed for the MMA materials under the three loading conditions, as shown in figure 4.6. No significant color change was noticed after 10,000 cycles, and only a 10 percent loss in color was recorded after 100,000 cycles for the three wheelsets. Such a small reduction in color could have been due to the presence of specific chemicals coupled with the thicker paint of the MMA materials. Furthermore, for the waterborne material (with or without glass beads), there was consistency in the rate of reduction under the three loading conditions, as shown in figures 4.7a and 4.7b. The change in color was obvious after 1,000 cycles (in some cases), which could have been due to thinner green waterborne paint in comparison to that of thermoplastic and the MMA paint materials.

In general, a gradual change in ΔL and ΔE_{ab} was observed throughout the laboratory experiments. The increase in the total color change (ΔEab) and lightness change (ΔL) were related to the loss in retroreflectivity. The ΔL of the pneumatic, scraper blade, and steel wheelset followed a trend similar to that of the ΔE_{ab} from 10,000 to 100,000 cycles. The MMA paint experienced the lowest color loss even after 100,000 cycles, irrespective of the exposure and the testing conditions. Also, it was observed that as the number of cycles of the pneumatic wheels increased, the color of each of the pavement markings darkened. The lightness loss could have been due to the appearance of the asphalt surface background because of the wearing of the pavement marking at the surface.

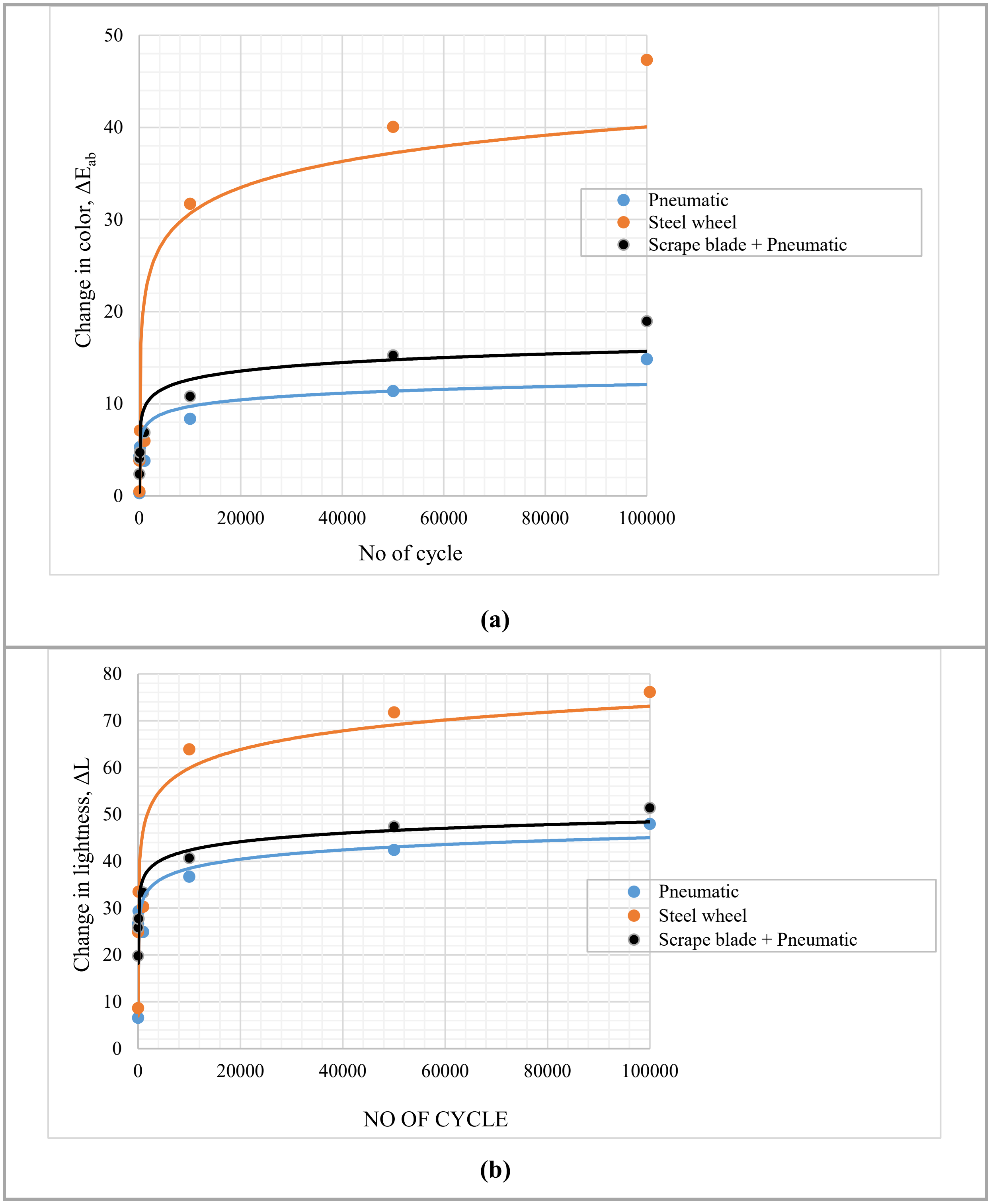

Figure 4.5. Changes of the thermoplastic material due to different loading conditions in (a) color; (b) lightness

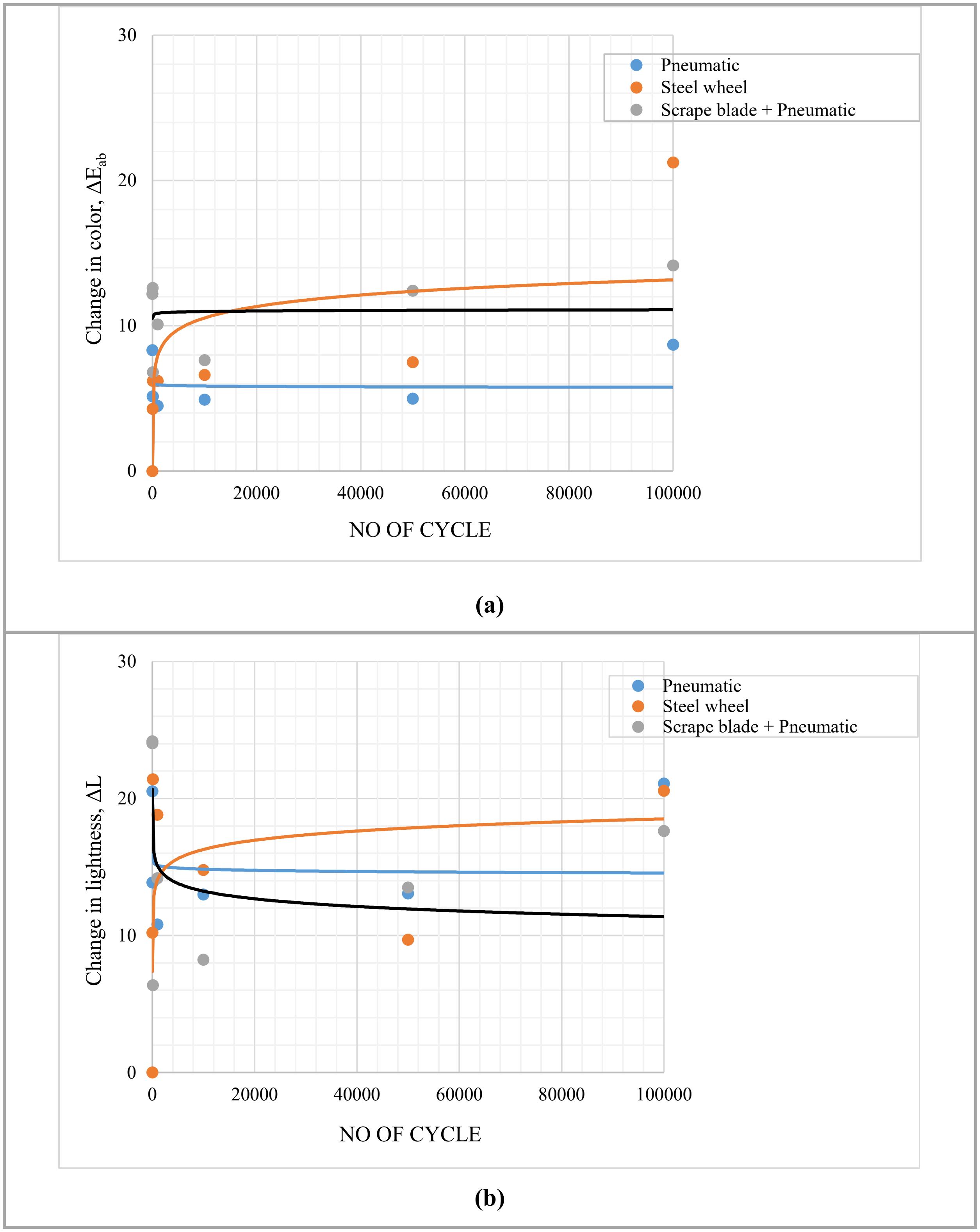

Figure 4.6. Changes of the MMA material due to different loading conditions in (a) color; (b) lightness

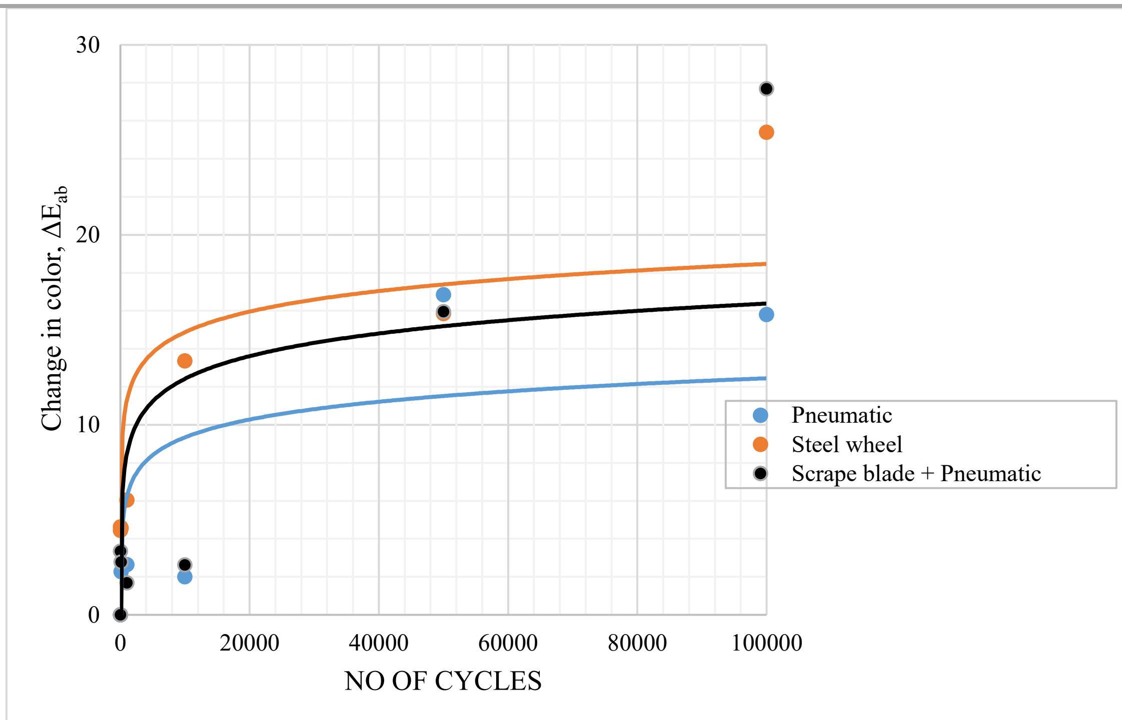

(a)

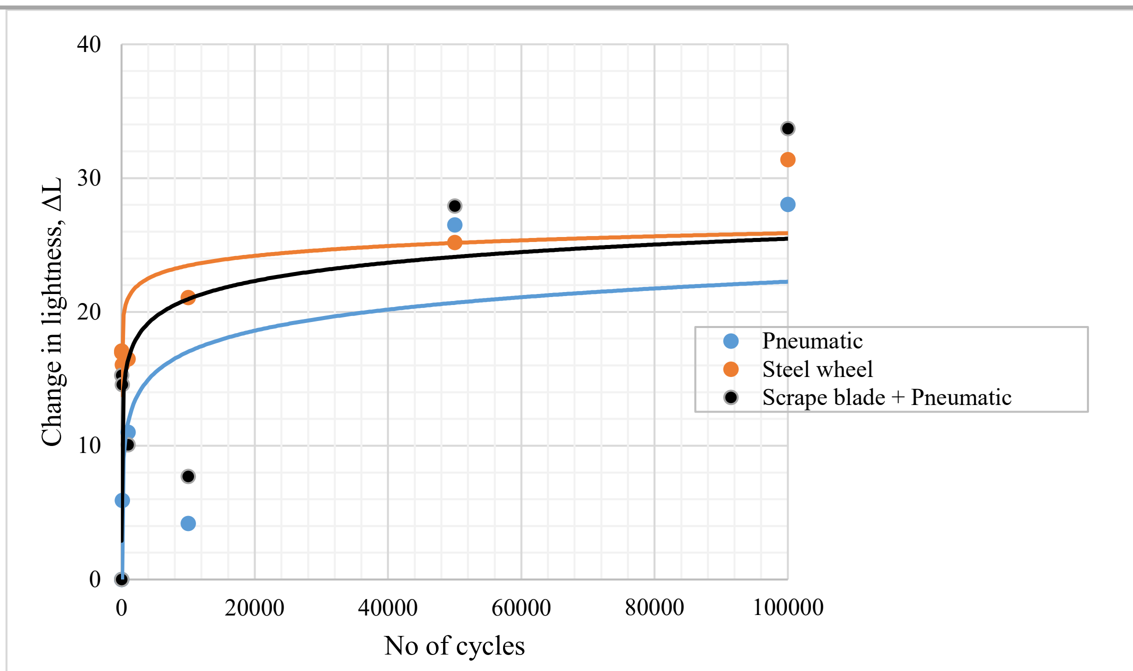

(b)

Figure 4.7. Changes of the waterborne (with glass beads) material due to different loading conditions in (a) color; (b) lightness

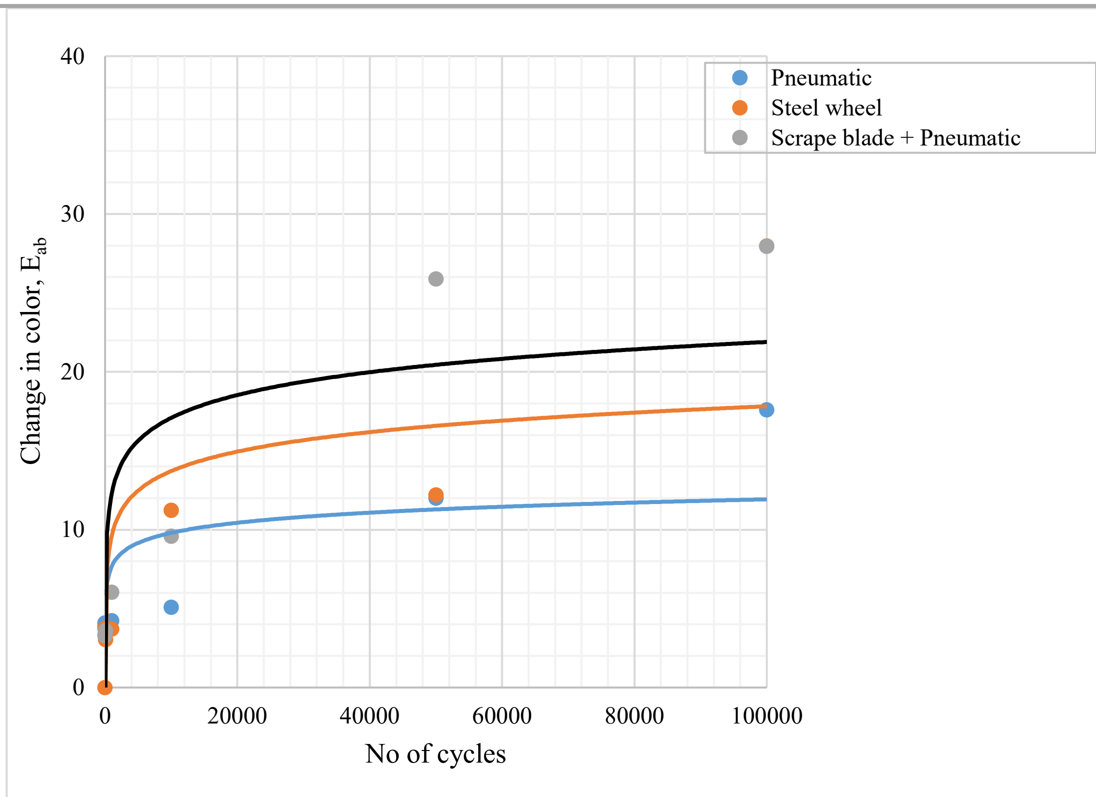

(a)

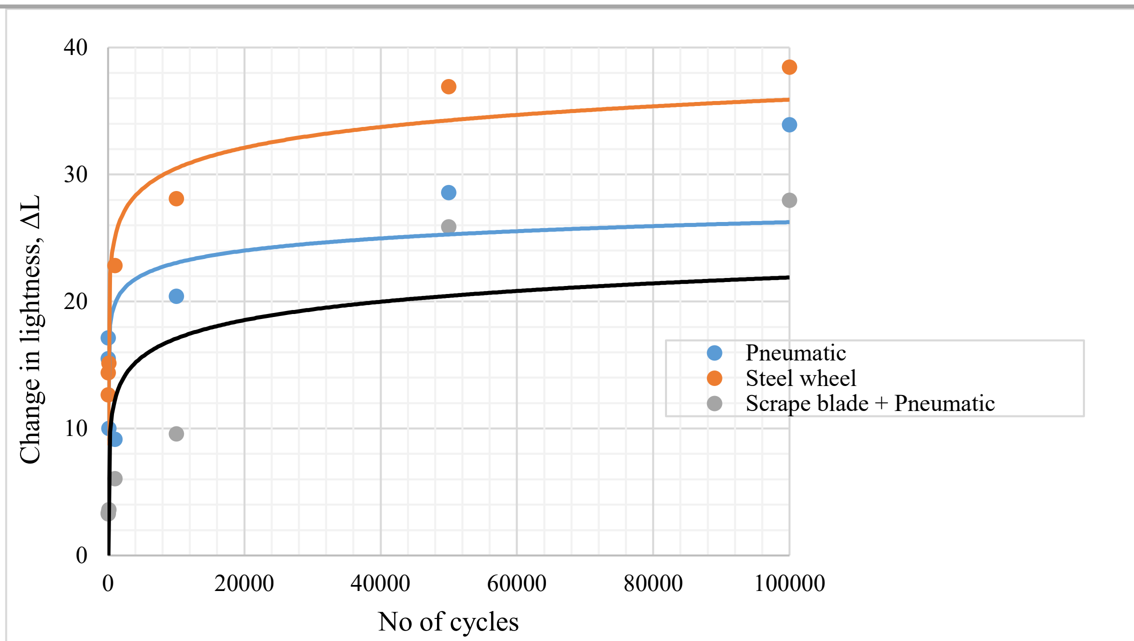

(b)

Figure 4.8. Changes of the waterborne (without glass beads) material due to different loading conditions in (a) color; (b) lightness

4.3. Durability of Pavement Markings

The research team evaluated the durability of pavement markings which refers to the ability of material to resist deterioration or withstand damage over time. One of the approaches used to measure pavement marking durability performance is to estimate the amount of remaining material at the surface over time. In this approach, the amount of material remaining on the pavement surface is measured with image analysis after the pavement marking specimens have been exposed to several physical activities. The durability of pavement markings is directly affected by traffic and the surrounding environment. In this study, "durability" was used as a performance measure to describe the material's response to a consistent mechanical motion produced by the TWPD that was intended to simulate the deterioration of pavement markings in the field (Mohamed et al. 2019).

An image analysis process employed a camera with high resolution and the ImageJ software to estimate the presence of material with the number of TWPD cycles. Digital images were taken by a camera mounted on a wooden stand in standard lighting conditions. Then, the software (ImageJ v.1.50i) was used to process the images and estimate the material loss and the surface texture change. In order to standardize the data collection, ASTM D6359-99 and ASTM D7585/D7585M were utilized as guidance standards. For consistency in the taking pictures, the camera was mounted at a fixed height under a fluorescent-light environment and several pictures were taken after each designated number of polishing cycles. This process has been discussed and used in previous studies (Mohamed et al. 2019 and 2020).

All pictures were processed with the software to estimate the material loss and percentage remaining. Figure 4.9 shows an example of image analysis in which the red and green colors in Image 1 and Image 2 represent the remaining material, while the black color refers to lost pavement marking materials. For analysis purposes, a durability rating procedure was used to estimate the remaining material percentage, where 0 percent indicated no material loss and 100 percent indicated complete material loss.

Figures 4.10, 4.11, and 4.12 show the results of the durability analysis of test marking materials under different operating conditions: pneumatic, scraper plate, and steel wheelsets, respectively. It was observed that for the waterborne paint (with and without glass beads), the markings peeled off the surface with increasing numbers of polishing cycles, unlike the MMA materials, which were polished and washed but did not peel off the surface. Therefore, the percentage of loss was calculated differently for the two materials (i.e., waterborne and MMA). The durability was calculated on the basis of the percentage of loss of the waterborne materials and on the percentage of polished area for the MMA materials.

The percentage of loss of the polished surface was plotted against the number of cycles. The trendline for most of the cases followed a power function except one case (i.e., the MMA under the pneumatic wheelset), which followed a logarithmic function. The coefficients of determination for the pneumatic, steel, and scraper blade ranged from 0.95 to 0.99.

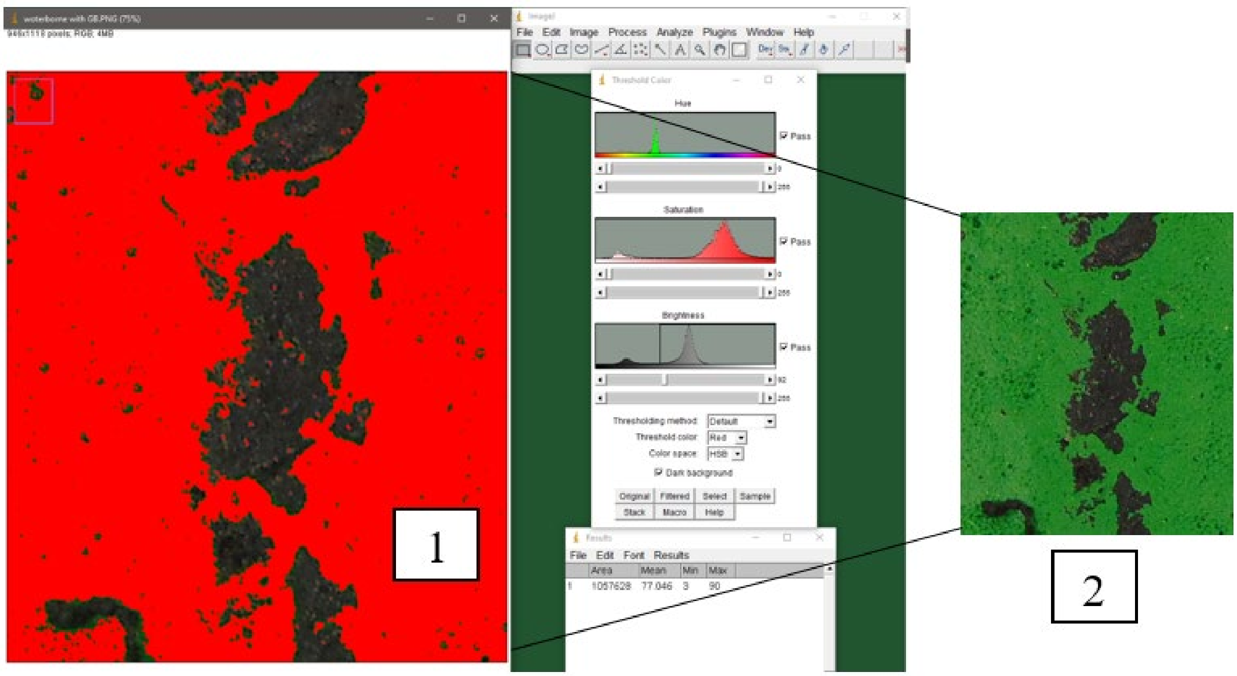

Figure 4.9. Durability calculation using ImageJ software

It has been observed that abraded rubber (eroded from the tire) is the element responsible for surface change, which in turn will affect measurements. Therefore, all substrates were carefully washed and cleaned before pictures were taken. During the installation of the MMA materials, the entire surface was covered with the marking material, and there weren’t gaps between the aggregates. During testing, for the MMA materials under the pneumatic wheelset, after 10,000 cycles the characteristics of surface texture started to change, and the green color started to lighten and turn white because of the washing and polishing. As a result, the MMA materials endured more TWPD loadings than the waterborne materials under the pneumatic and scraper plate wheelsets (figures 4.10 and 4.11). In the meantime, under the steel wheelset there was no significant difference between the waterborne and MMA materials after 100,000 cycles (figure 4.12). This could have been due to the harsh loading conditions of the steel wheelset. Note that there was no noticeable loss of thermoplastic material under different loading conditions.

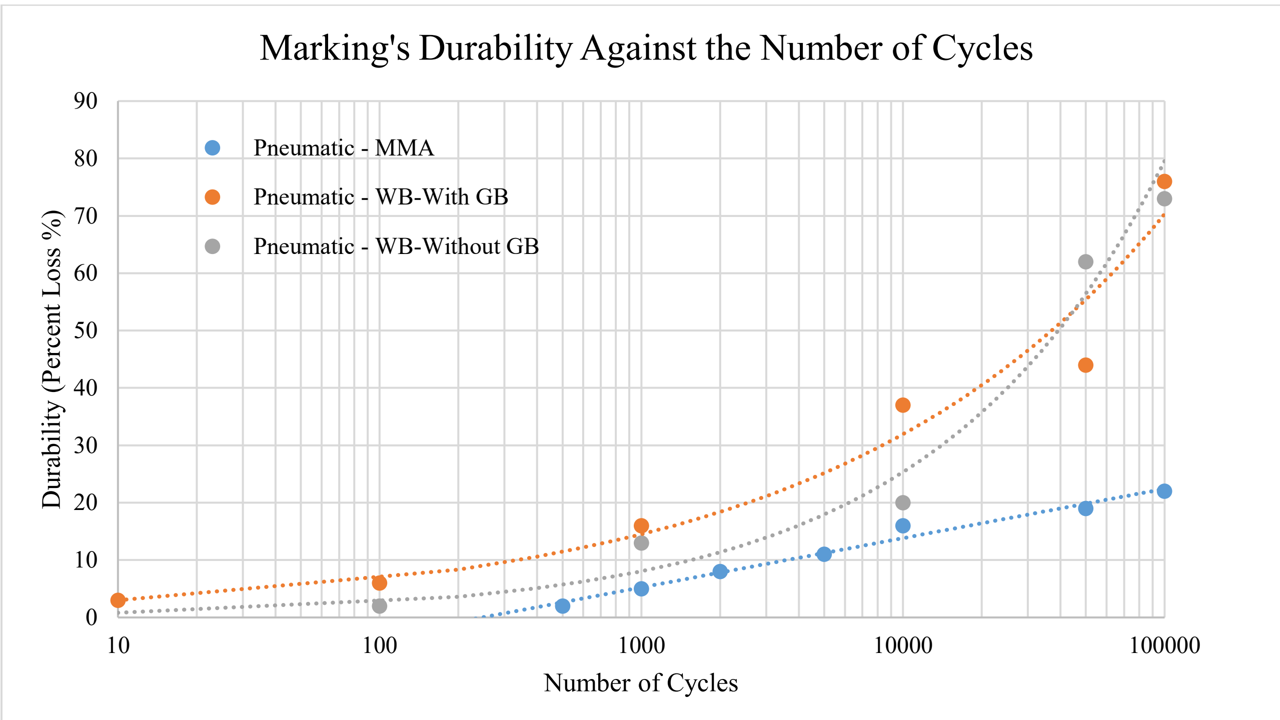

Figure 4.10. Durability of test markings under the pneumatic wheelset.

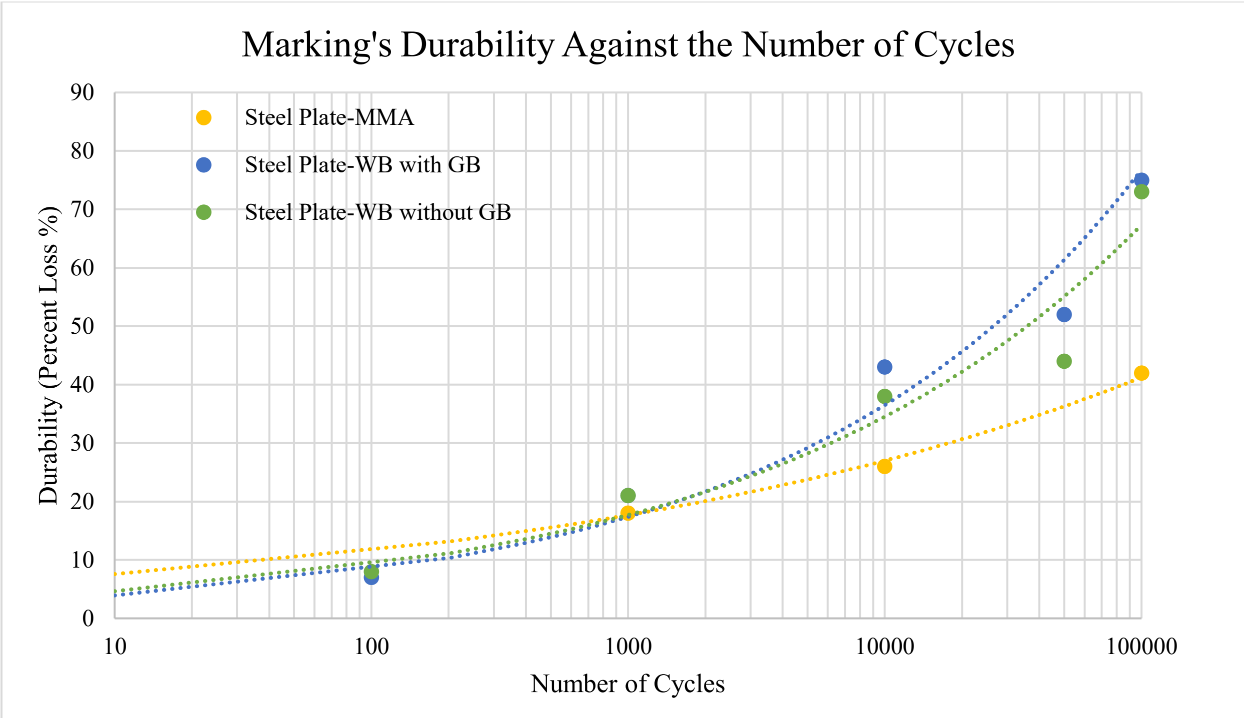

Figure 4.11. Durability of test markings under the scraper plate wheelset.

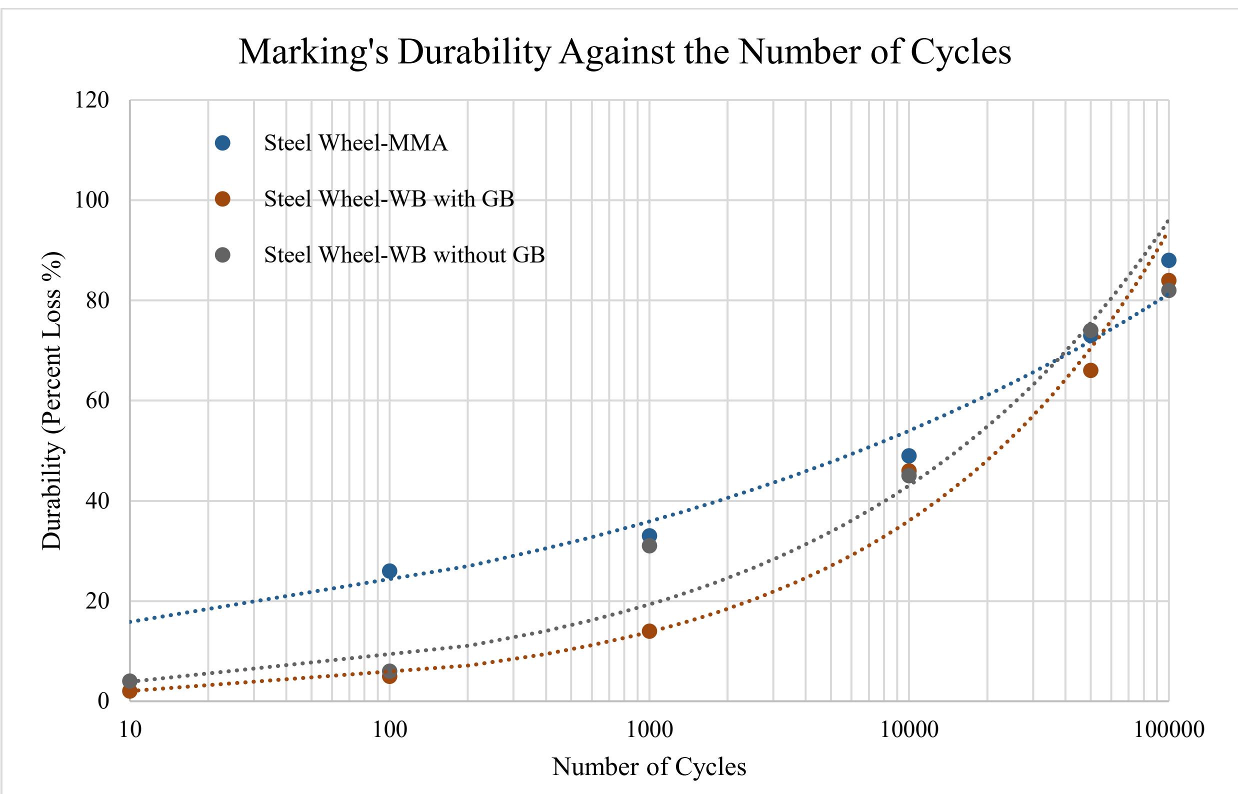

Figure 4.12. Durability of test markings under the steel wheelset.

Table 4.3. Durability models and R^2 under each TWPD wheelset

Pavement Marking Type	Pneumatic - MMA	Pneumatic - WB-With GB	Pneumatic - WB-Without GB
Equation	$y = 3.7334\ln(x) - 20.562$	$y = 1.36x^{0.3427}$	$y = 0.2599x^{0.4973}$
R^2	0.98	0.99	0.96
Pavement Marking Type	**Steel Plate-MMA**	**Steel Plate-WB with GB**	**Steel Plate-WB without GB**
Equation	$y = 4.9569x^{0.184}$	$y = 1.8664x^{0.3228}$	$y = 2.3778x^{0.2904}$
R^2	0.99	0.97	0.96
Pavement Marking Type	**Steel Wheel-MMA**	**Steel Wheel-WB with GB**	**Steel Wheel-WB without GB**
Equation	$y = 10.521x^{0.1776}$	$y = 0.7805x^{0.4162}$	$y = 1.7411x^{0.3484}$
R^2	0.97	0.99	0.95

4.4. Surface Friction Characteristics

Figure 4.13 shows the mean texture depth (MTD) for the test substrates with different markings materials. The thermoplastic substrates had a relatively higher texture than the waterborne and MMA substrates. The thermoplastic had higher irregularities than the other surfaces, which resulted in a higher macrotexture or MTD.

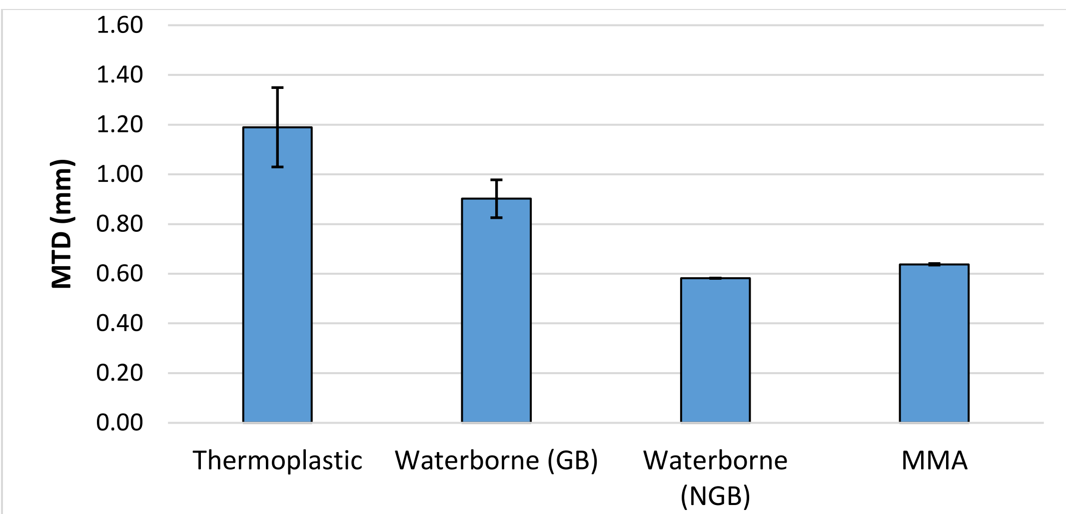

Figure 4.13. Mean texture depth (MTD) for the test surfaces

Figures 4.14 to 4.16 show the International Friction Index (IFI) at different numbers of loading cycles for the MMA, thermoplastic, and waterborne marking materials, respectively. The results revealed that the MMA surfaces had the highest friction, whereas the thermoplastic had the lowest friction. A higher IFI is associated with better traction and less slippery surfaces in wet conditions. The IFI decreased with the number of cycles under different loading conditions (pneumatic, scraper plate, and steel wheel set) for the MMA. This was due to polishing of the surface. The IFI didn't change much with the number of cycles for the thermoplastic surfaces, as the thermoplastic materials had not been worn or polished even after the terminal number of loading cycles (i.e., 100,000 cycles). Interestingly, the IFI for the waterborne material increased slightly with number of cycles, and this could have been due to a loss of the waterborne paint and exposure of the asphalt surface underneath the paint, which had higher friction than the paint.

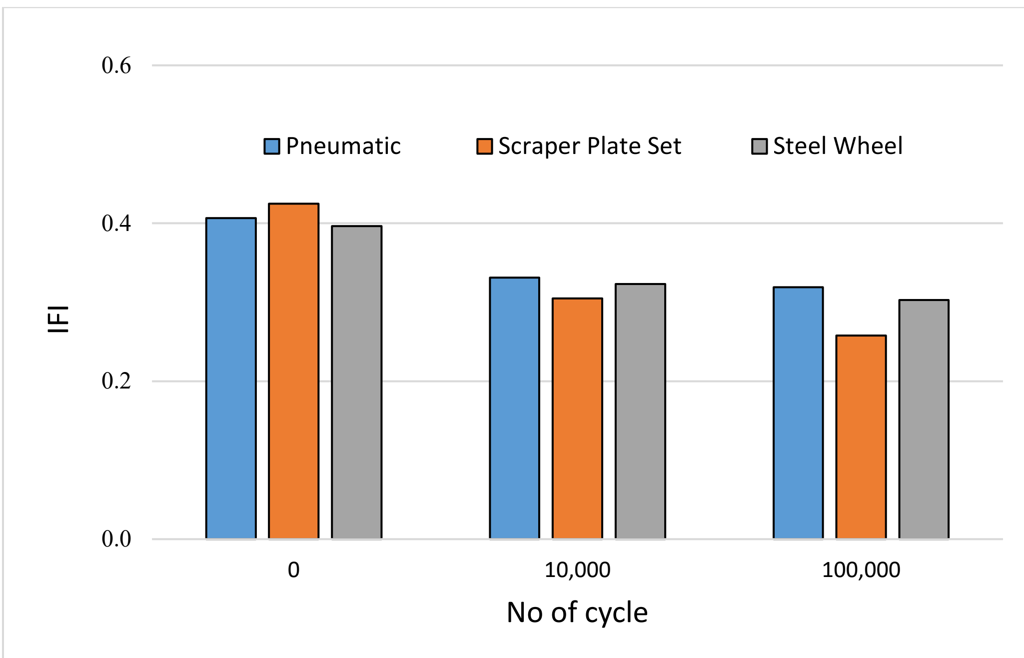

Figure 4.14. International Roughness Index (IFI) with number of loading cycles for the MMA materials

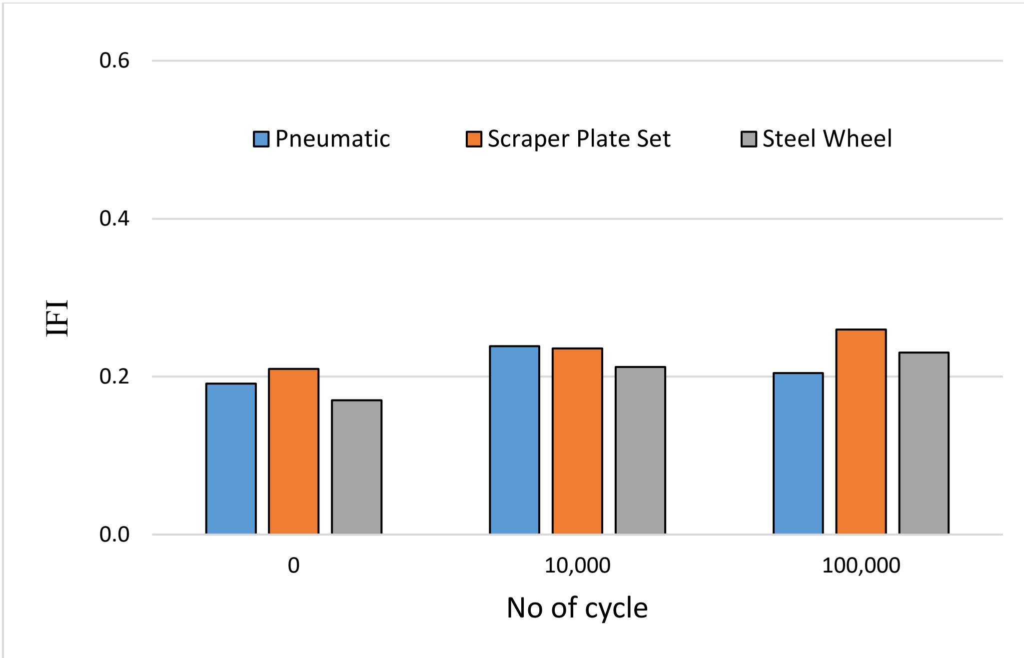

Figure 4.15. International Roughness Index (IFI) with number of loading cycles for the thermoplastic materials

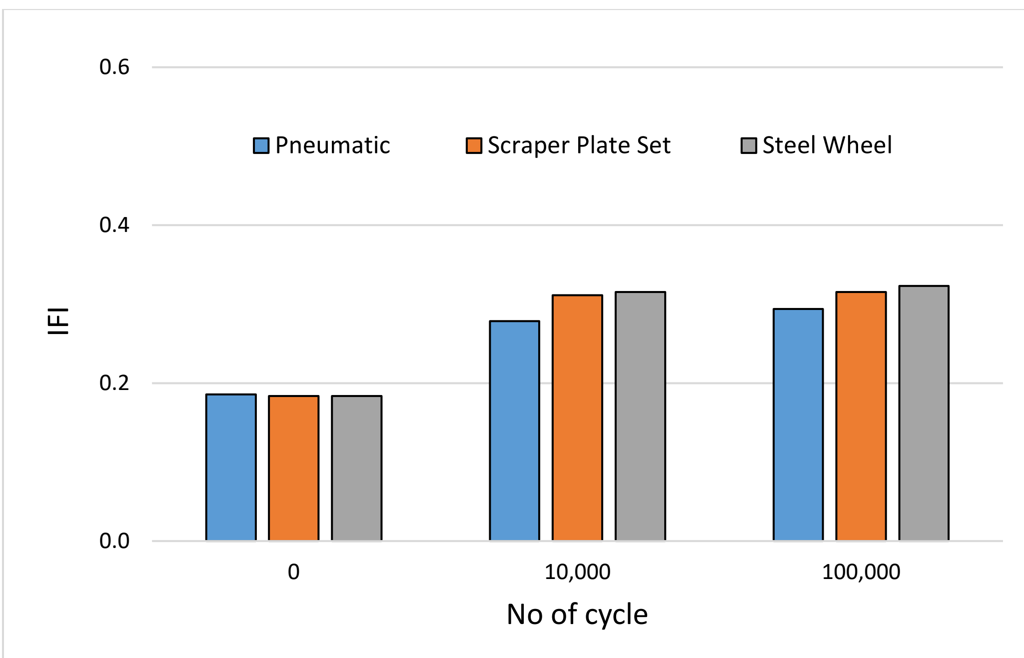

Figure 4.16. International Roughness Index (IFI) with number of loading cycles for the waterborne materials

CHAPTER 5. Conclusions

This study used a new method to evaluate pavement marking deterioration for bike lanes. Three paint products were tested: 1) green waterborne paint, 2) green liquid methacrylate (MMA) paint, and 3) white thermoplastic paint. The research team prepared substrates of asphalt mixtures with the paint products for testing. A three-wheel polishing device was used to polish the test substrates with pneumatic tires, steel wheels, and a steel scraper blade. The pneumatic tires simulated traditional motor vehicle traffic. The steel wheel simulated a more abrasive condition representative of maintenance equipment. The steel scraper blade was developed and proposed to simulate the deterioration of the pavement surface due to snowplowing operations.

The research team measured various characteristics to assess the performance and durability of the test bike lane pavement markings. The characteristics were measured after each set of polishing cycles. These characteristics included durability, retroreflectivity, color changes, and friction of the test materials. The retroreflectivity was measured in dry and wet conditions.

The main findings of these research study can be summarized as follows:

- As expected, the retroreflectivity decreased with the number of polishing cycles. Overall, there was a significant decrease in percentage of retroreflectivity after 1,000 cycles for all testing conditions before retroreflectivity reached a terminal value. These results were consistent with field observations reported in the literature.
- The steel wheels were found to cause a more significant drop in retroreflectivity for the thermoplastic than the other testing conditions (e.g., pneumatic tires and scraper blade).
- The loss in retroreflectivity for the MME materials followed a trend similar to that of the thermoplastic materials.
- The retroreflectivity of the waterborne paint with glass beads decreased less than that of the waterborne paint without glass beads.
- The logarithmic model was found to describe the change in the retroreflectivity in relation to the number of loading cycles with high R^2 values for all the retroreflectivity data sets.
- The MMA paint experienced the lowest color loss even after 100,000 cycles, irrespective of the exposure and the testing conditions. It is believed that the small reduction in color was due to the presence of specific chemicals, coupled with the

thicker paint of the MMA materials in comparison to the thickness of the waterborne materials.

- The durability results demonstrated that the waterborne markings peeled off the surface with increasing numbers of polishing cycles, unlike the MMA materials, which were polished and washed but did not peel off the surface.
- The MMA materials endured more TWPD loadings than the waterborne materials under the pneumatic and scraper plate wheelsets. However, there was no significant difference under the steel wheels.
- The friction results demonstrated that that the MMA surfaces had the highest friction, whereas the thermoplastic had the lowest friction.

The results showed that the laboratory evaluation procedure can be standardized and used as a pre-qualifying test to assess different pavement marking products or select a suitable material from a set of alternatives for a specific climate or operational conditions. This procedure is considered to be flexible because it has room to test the pavement markings under different environments (e.g., cold, hot, rainy, or snowy) and types of traffic loads (e.g., different types of tires, steel wheels, and studded tires). It is also advantageous because it is less expensive, easier to perform, and reduces the testing time from years (based on field observations) to days (if conducted in the laboratory).

References

Aldagari, S., Al-Assi, M., Kassem, E., Chowdhury, A. and Masad, E., 2018. *Prediction Models for Skid Resistance of Asphalt Pavements and Seal Coat* (No. 18-05541).

ASTM (American Society for Testing and Materials). 2016. Standard practice for calculation of color tolerances and color differences from instrumentally measured color coordinates. ASTM D2244-16. West Conshohocken, PA: ASTM

Beautru, Y., Kane, M., Cerezo, V. and Do, M.T., 2011, June. Effect of thin water film on tire/road friction. In *Young Researchers Seminar (YRS 2011)* (p. 19p).

Carlson, Paul, Eun-Sug Park, Adam Pike, R.J. Porter, Jeffrey Miles, Bryan Boulanger, Omar Smadi, Neal Hawkins, Seth Chalmers, Frank Darmiento, Adrian Burde, Beverly Kuhn, Wendy Ealding, 2013. Pavement Marking Demonstration Projects: State of Alaska and State of Tennessee (No. FHWA-HRT-12-048).

Craig, W.N., Sitzabee, W.E., Rasdorf, W.J., Hummer, J.E., 2007. Statistical validation of the effect of lateral line location on pavement marking retroreflectivity degradation. Public Works Manag. Policy 12, 431–450.

FHWA, 2015. FHWA Guidance: Bicycle and Pedestrian Provisions of Federal Transportation Legislation [WWW Document]. URL https://www.fhwa.dot.gov/environment/bicycle_pedestrian/guidance/guidance_2015.cfm (accessed 8.11.20).

Gibbons, R., Williams, B. and Cottrell Jr, B.H., 2013. *Assessment of the Durability of Wet Night Visible Pavement Markings: Retroreflectivity Experiment* (No. 13-3799).

Hales, C., Rhodes, V., Birk, M., Burchfield, R., Flecker, J., Hunter, W.W., Harkey, D.L., Stewart, J.R., 1999. CITY OF PORTLAND, OFFICE OF TRANSPORTATION 24.

Hunter, W., 2008. Evaluation of a Green Bike Lane Weaving Area in St. Petersburg, Florida (Technical Report).

Jiang, Y., 2008a. Durability and retro-reflectivity of pavement markings (synthesis study) (Final Report No. FHWA/IN/JTRP-2007/11). Joint Transportation Research Program, Indiana.

Jiang, Y., 2008b. Durability and retro-reflectivity of pavement markings (synthesis study). Jt. Transp. Res. Program 235.

Kane, M., Rado, Z. and Timmons, A., 2015. Exploring the texture–friction relationship: from texture empirical decomposition to pavement friction. *International Journal of Pavement Engineering*, *16*(10), pp.919-928.

Koetsier, L.S., 2016. Colored Pavement for Bicycle Facilities in Oklahoma (Technical Report No. 73105).

Kopf, J. (2004). Reflectivity of pavement markings: Analysis of retroreflectivity degradation curves (No. WA-RD 592.1,). Olympia: Washington State Department of Transportation.

MacNaughton, P., Melly, S., Vallarino, J., Adamkiewicz, G., Spengler, J.D., 2014. Impact of bicycle route type on exposure to traffic-related air pollution. Sci. Total Environ. 490, 37–43. https://doi.org/10.1016/j.scitotenv.2014.04.111

Migletz, J., Graham, J., Harwood, D., Bauer, K., 2001. Service life of durable pavement markings. Transp. Res. Rec. J. Transp. Res. Board 13–21.

Migletz, J. and Graham, J.L., 2002. *Long-term pavement marking practices: A synthesis of highway practice* (Vol. 306). Transportation Research Board.

Miles, J.D., Carlson, P.J., Eurek, R., Re, J. and Park, E.S., 2010. *Evaluation of potential benefits of wider and brighter edge line pavement markings* (No. FHWA/TX-10/0-5862-1). Texas Transportation Institute.

Mohamed, M., Abdel-Rahim, A., Kassem, E., Chang, K., McDonald, A.G., 2020. Laboratory-Based Evaluation of Pavement Marking Characteristics. J. Transp. Eng. Part B Pavements 146, 04020016. https://doi.org/10.1061/JPEODX.0000168

Mohamed, M., Skinner, A., Abdel-Rahim, A., Kassem, E., Chang, K., 2019. Deterioration Characteristics of Waterborne Pavement Markings Subjected to Different Operating Conditions. J. Transp. Eng. Part B Pavements 145, 04019003. https://doi.org/10.1061/JPEODX.0000101

Moser, Johnson, Jeff Morey, Bruce Daniel, Wayne Lindblom, 2015. MnDOT Pavement Marking Field Guide.

MUTCD, 2009. MUTCD 2009 [WWW Document]. URL https://mutcd.fhwa.dot.gov/htm/2009/part3/part3a.htm (accessed 8.11.20).

NACTO, 2012. Colored Pavement Material Guidance [WWW Document]. NACTO. URL https://nacto.org/publication/urban-bikeway-design-guide/bikeway-signing-marking/colored-pavement-material-guidance/ (accessed 8.11.20).

Parker, N.A. and Meja, M.S., 2003. Evaluation of performance of permanent pavement markings. *Transportation Research Record*, *1824*(1), pp.123-132.

Schalkwyk, I. van, 2010. Enhancements to Pavement Marking Testing Procedures (Final Report No. FHWA-OR-RD-11-02). Oregon Department of Transportation, Oregon.

Saito, K., Horiguchi, T., Kasahara, A., Abe, H. and Henry, J.J., 1996. Development of portable tester for measuring skid resistance and its speed dependency on pavement surfaces. *Transportation Research Record*, *1536*(1), pp.45-51.

Smadi, O., 2013. *Predicting the initial retroreflectivity of pavement markings from glass bead quality* (Vol. 743). Transportation Research Board.

Timothy, J., Gates, H., Gene Hawkins, J., Elisabeth R, R., 2003. Effective Pavement Marking Materials and Applications for Portland Cement Concrete Roadways (No. 4150–2). Texas Transportation Institute, Texas.

Tumlin, J., 2012. Sustainable Transportation Planning: Tools for Creating Vibrant, Healthy, and Resilient Communities. John Wiley & Sons, Incorporated, New York, UNITED STATES.

Adminstration, F.H., 2011. Manual on Uniform Traffic Control Devices (MUTCD). *USD o. Transportation, ed., FHWA, FHWA, Washington, DC*.

Wang, S., 2010. Comparative Analysis of NTPEP Pavement Marking Performance Evaluation Results. University of Akron.

Zhang, G., Hummer, J.E. and Rasdorf, W., 2010. Impact of bead density on paint pavement marking retroreflectivity. *Journal of Transportation Engineering*, *136*(8), pp.773-781.

Zhang, Y. and Wu, D., 2010, October. Methodologies to predict service lives of pavement marking materials. In *Journal of the Transportation Research Forum* (Vol. 45, No. 3).